6 Modelling catalytic oxidation

6.1 Observed catalytic behaviour

In Chapter 4 (the microstructural investigation) it was briefly mentioned that the actions of metallic catalysts are readily noticeable during the SEM examination of the oxidised graphite particles. In this chapter some of these observed behaviours are examined in more detail. Based on this investigation, two approaches to modelling the effect of catalytic impurities will be explored.

As mentioned in the previous chapter, the catalytic behaviours examined in this chapter are limited to those present on the RFL graphite, i.e. as-received (RFL), partially purified (PPRFL) and contaminated (CPRFL). This allows a continuation of the fundamental modelling approach applied in the previous chapter to this ideal model graphite. On a macroscopic level the edge effects of catalytic particles during oxidation are immediately visible, as illustrated by Figure 6-1 to Figure 6-3. These present visually at a distance as a fine roughening of the edges.

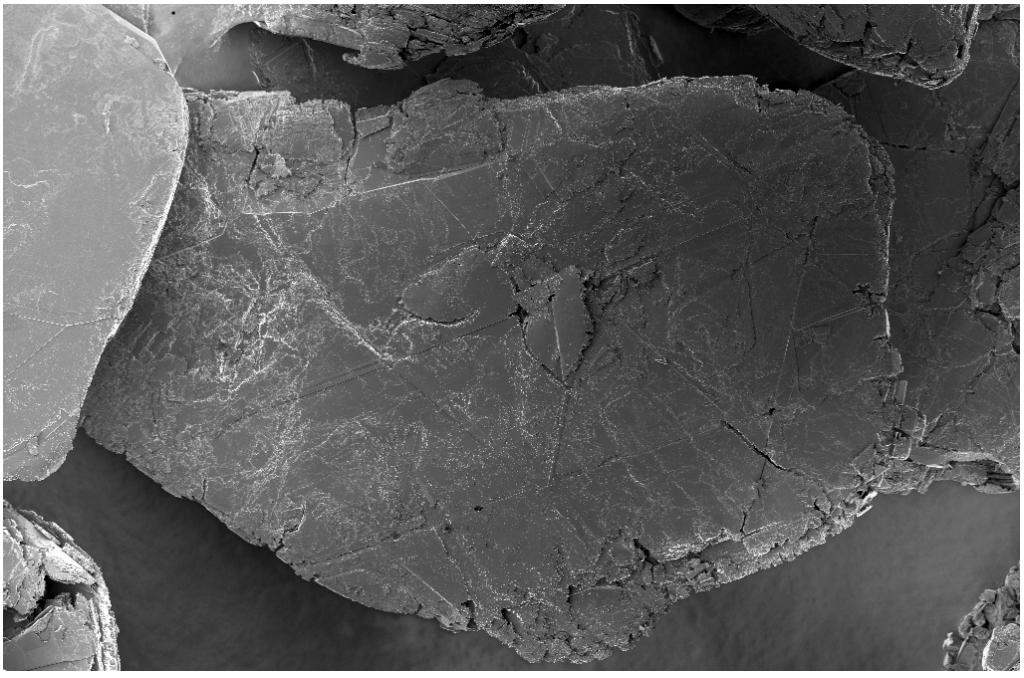

Figure 6-1: Example 1 of edge-roughening effect (500x magnification)

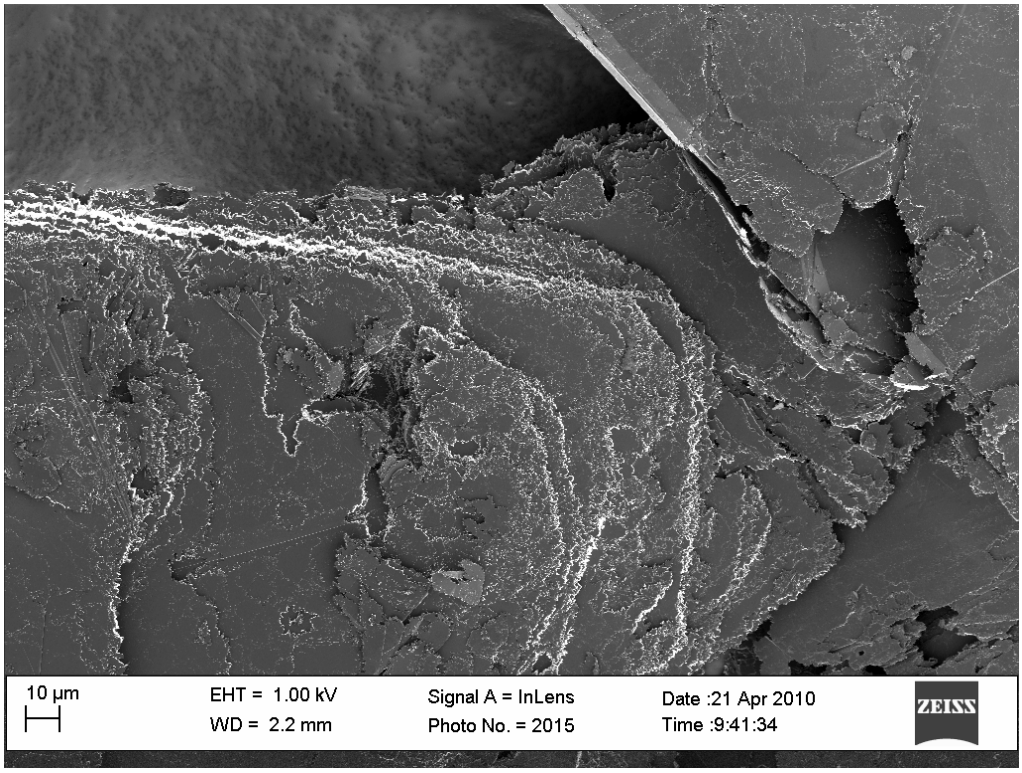

Figure 6-2: Example 2 of edge-roughening effect (1 000x magnification)

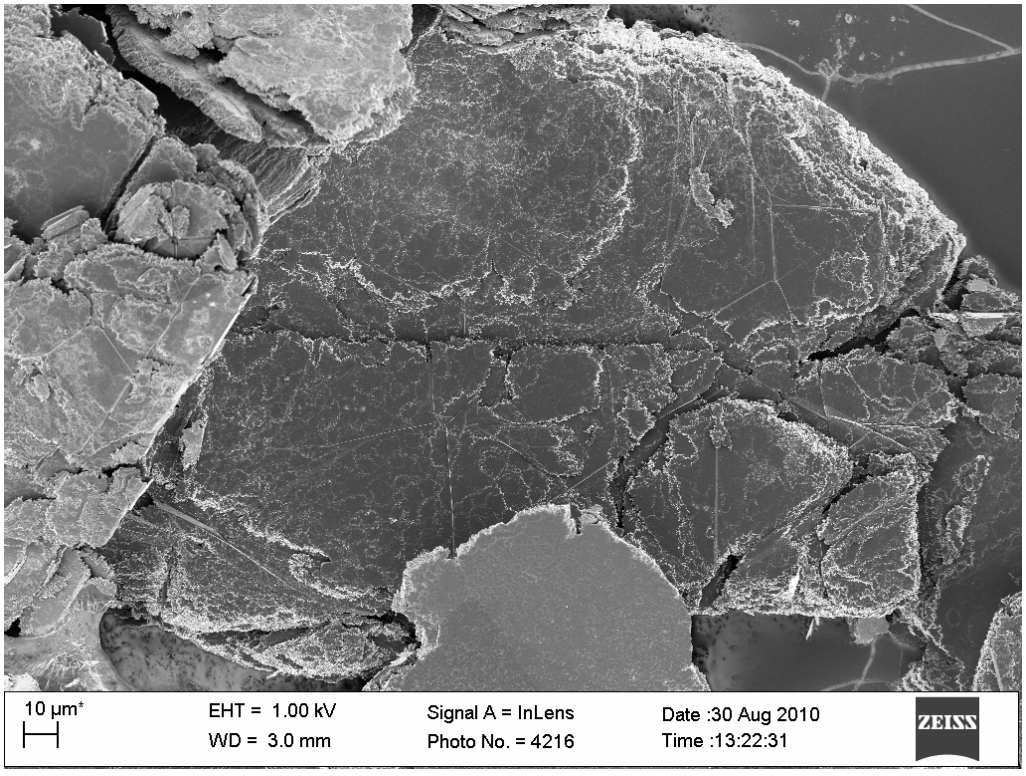

Figure 6-3: Example 3 of edge-roughening effect (1 000x magnification)

From these macroscopic views it is evident that channel penetration into the sample is fairly limited. The influence of these catalysts is mainly localised at, or a short distance from, the flake edge or at basal steps. Overall, the bulk flakes appear to be intact. When these edges are examined more closely, the highly erratic channels that create them become discernible. This is illustrated by the two series of progressively increasing magnification in Figure 6-4 to Figure 6-7 and Figure 6-8 to Figure 6-11, for RFL and CPRFL respectively.

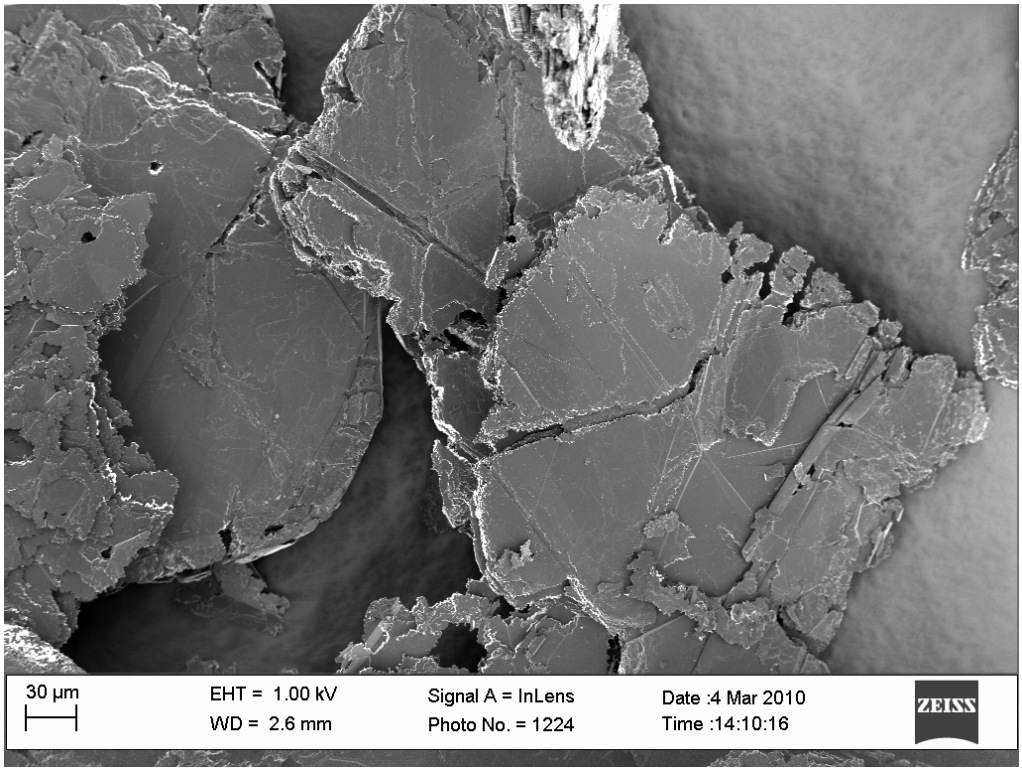

Figure 6-4: Series 1 RFL edge-roughening effect (500x magnification)

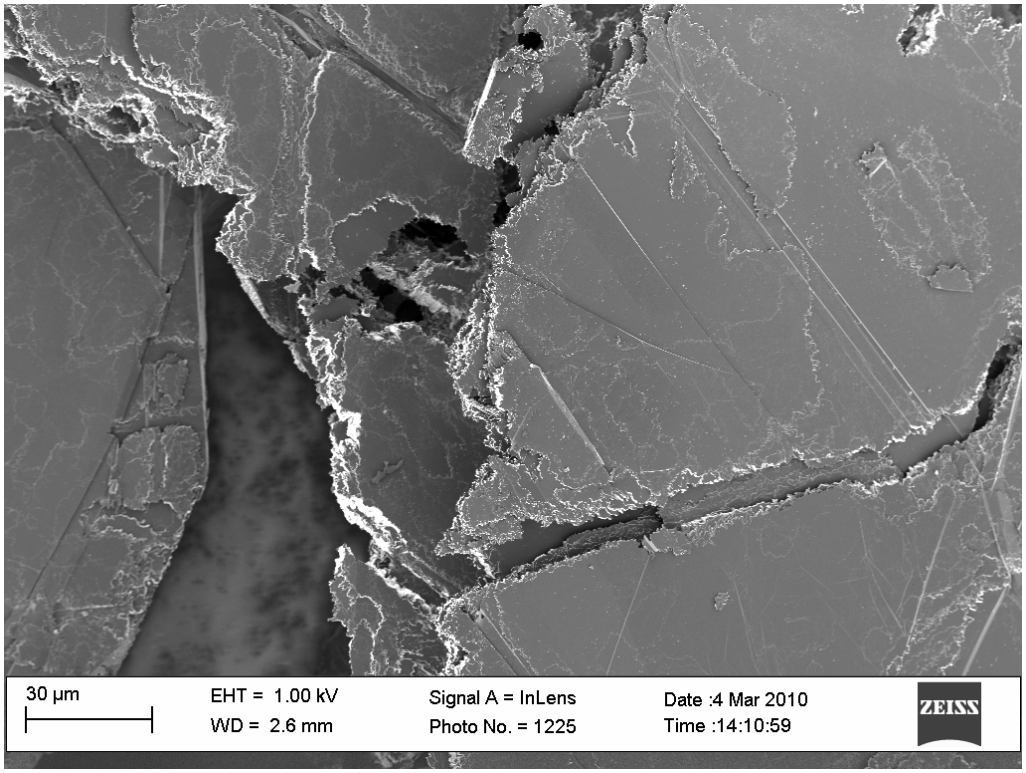

Figure 6-5: Series 1 RFL edge-roughening effect (1 000x magnification)

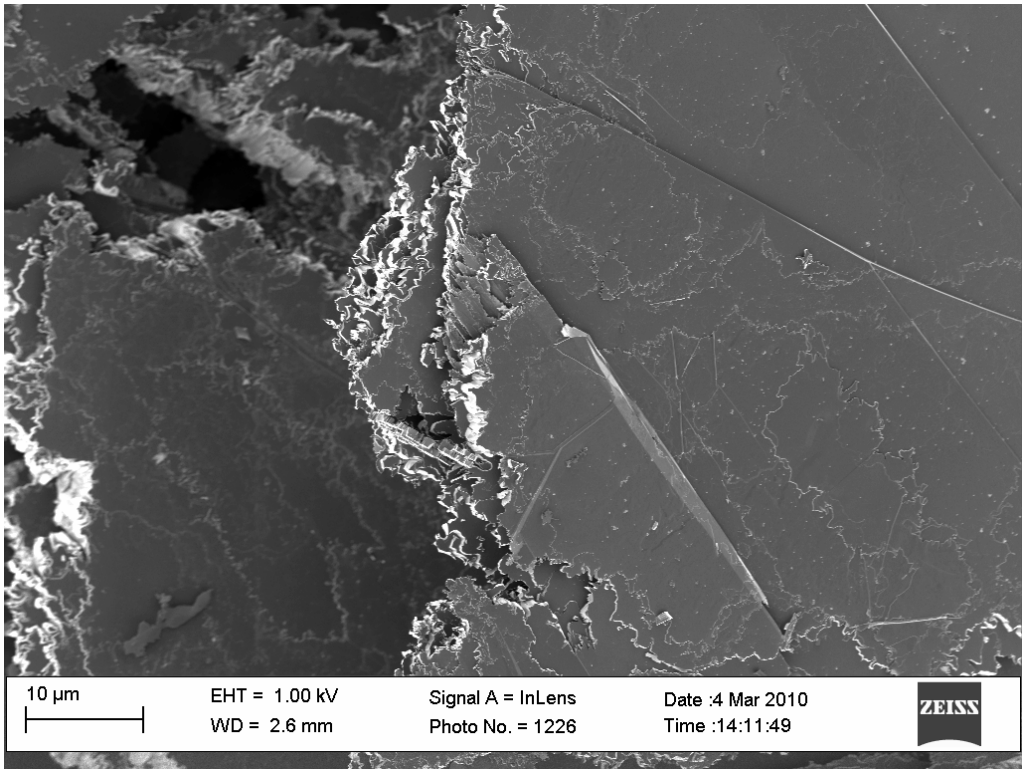

Figure 6-6: Series 1 RFL edge-roughening effect (3 000x magnification)

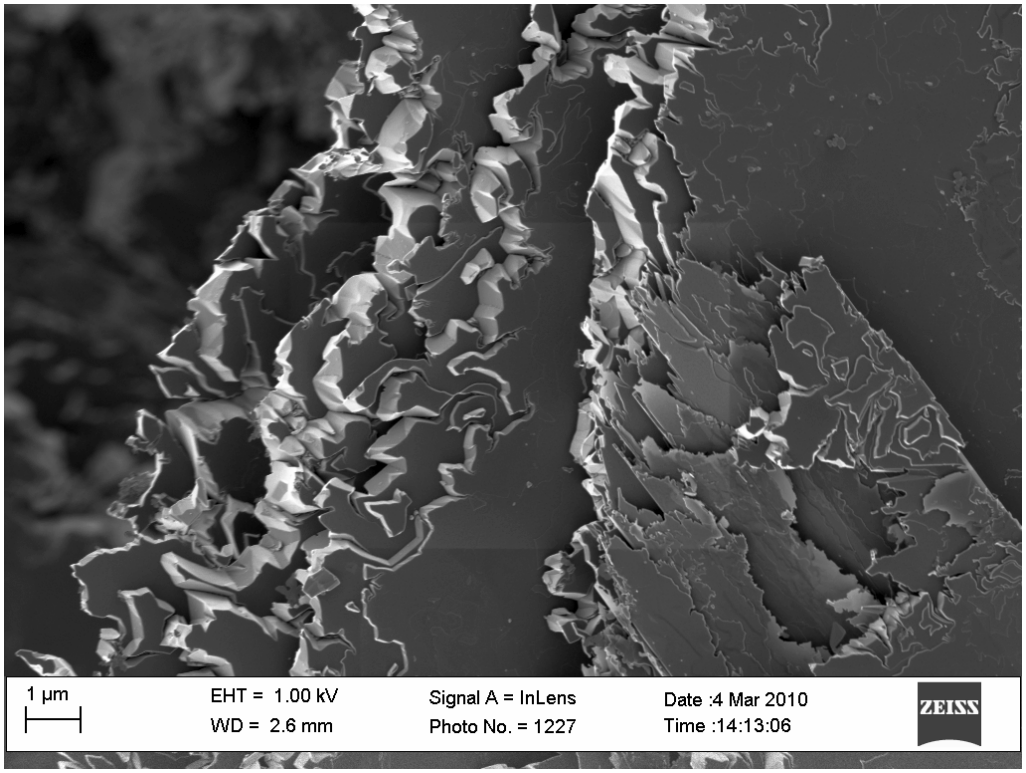

Figure 6-7: Series 1 RFL edge-roughening effect (16 000x magnification)

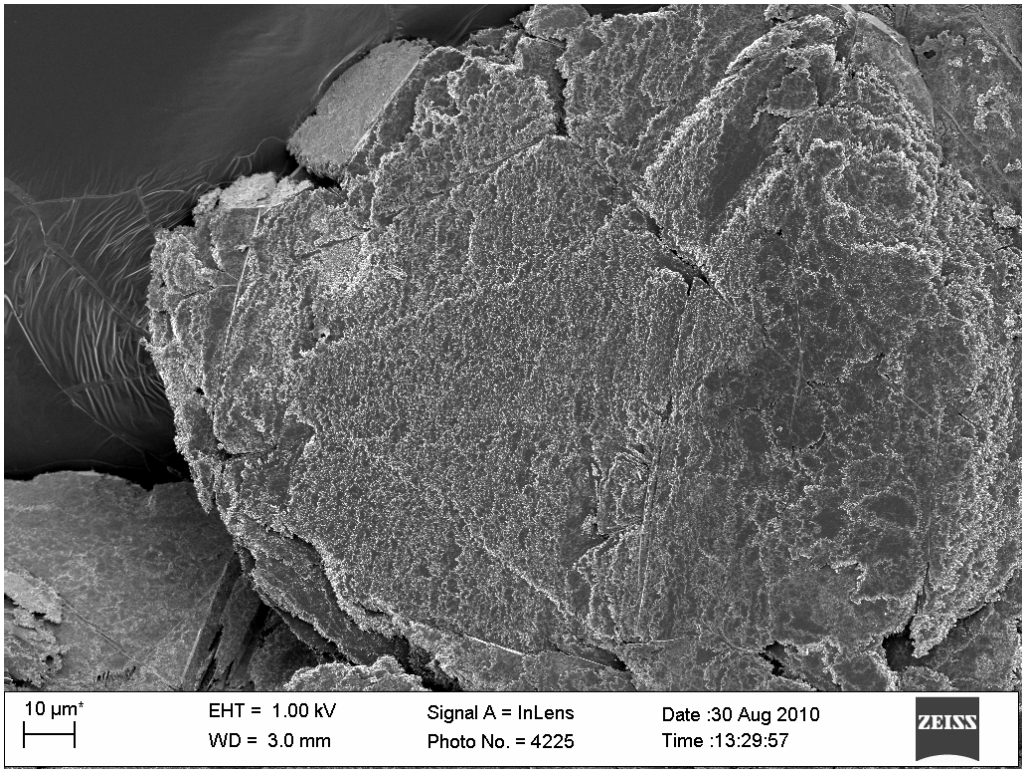

Figure 6-8: Series 2 CPRFL edge-roughening effect (1 500x magnification)

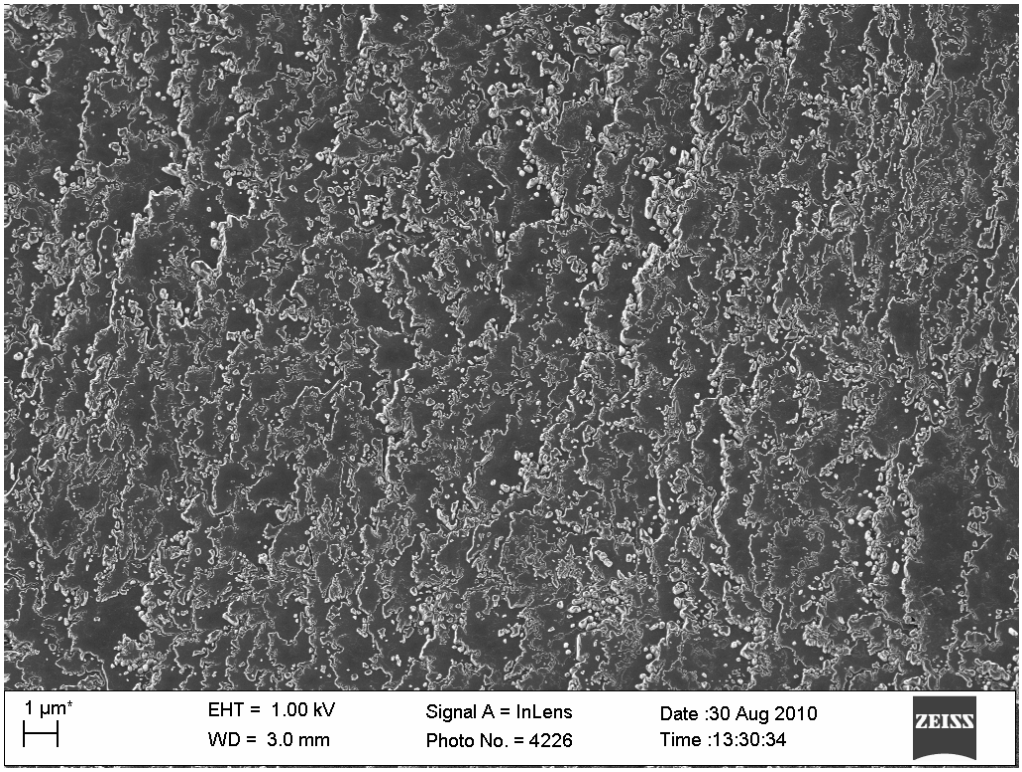

Figure 6-9: Series 2 CPRFL edge-roughening effect (10 000x magnification)

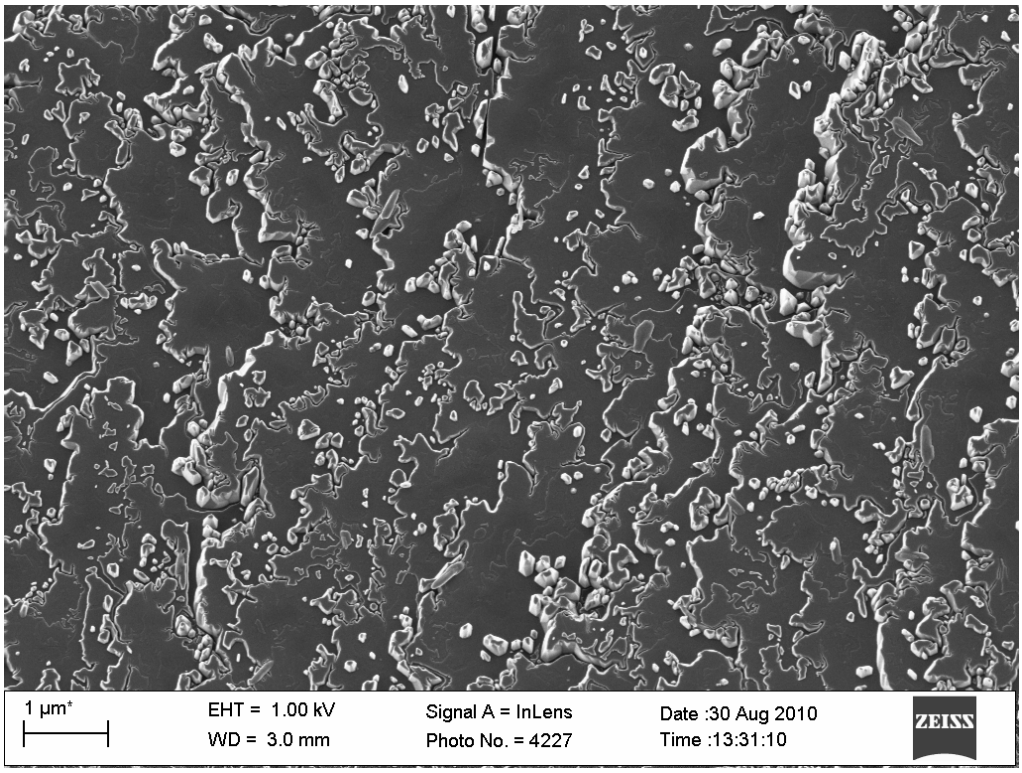

Figure 6-10: Series 2 CPRFL edge-roughening effect (25 000x magnification)

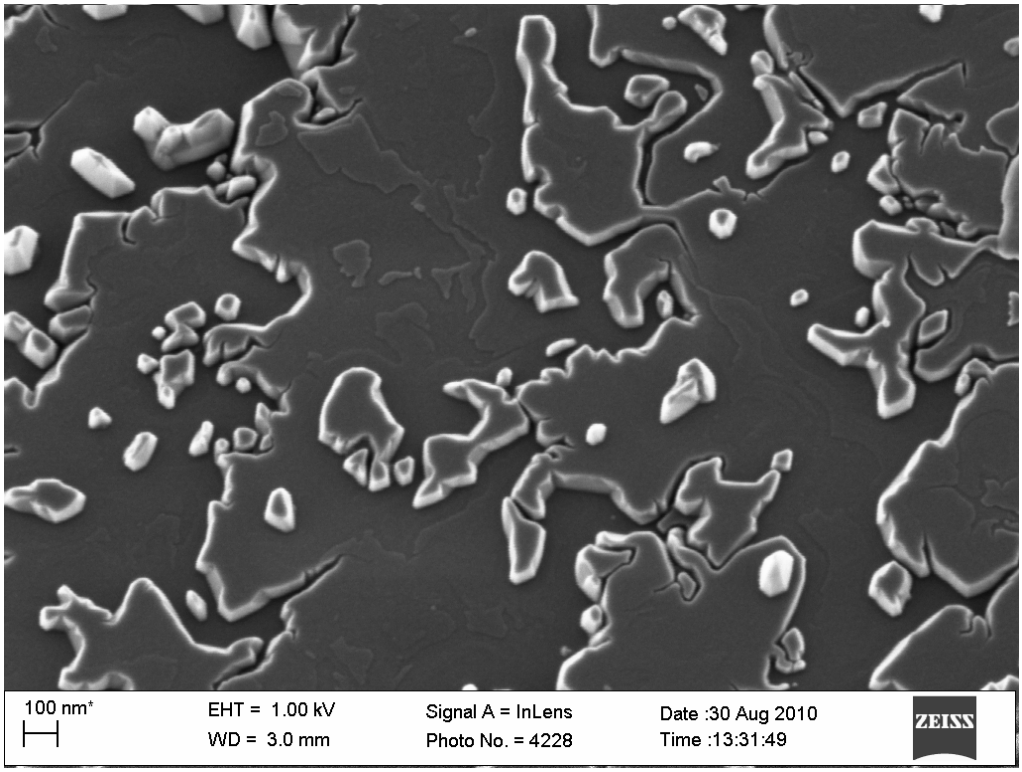

Figure 6-11: Series 2 CPRFL edge-roughening effect (100 000x magnification)

The individual channels only become discernible at very high magnitudes and are of the order of a few hundred nanometres. Despite the as-received RFL graphite containing less than 1 000 ppm impurities, the effect of the catalyst seems to be fairly homogeneous and well dispersed along the edges and steps of even the larger and thicker flakes, as is typified by Figure 6-12 and Figure 6-13.

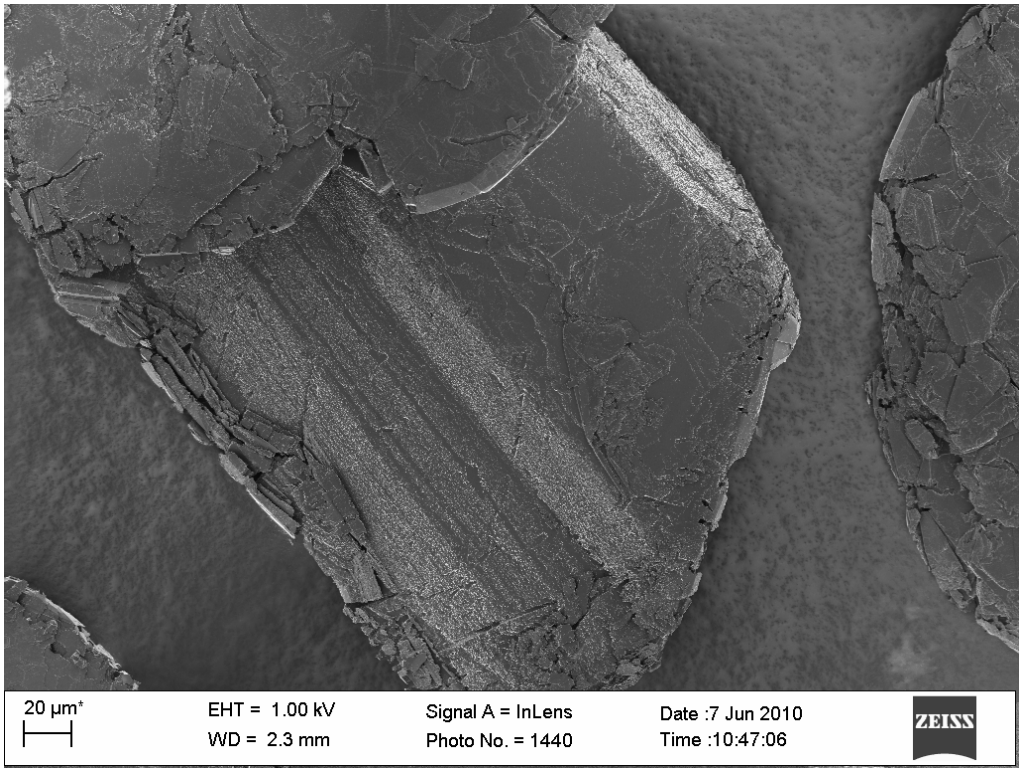

Figure 6-12: Catalyst edge dispersion (800x magnification)

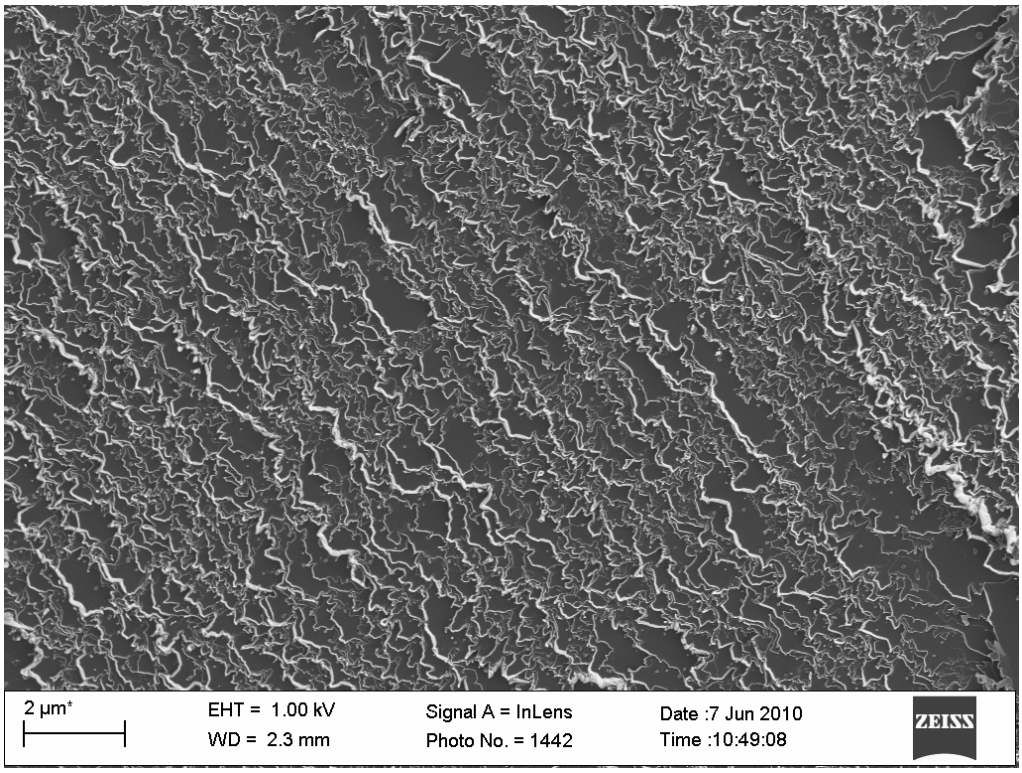

Figure 6-13: Catalyst edge dispersion (15 000x magnification)

When regions of slightly lower catalytic activity are examined, a variety of different behaviours can be distinguished. It is sensible to refer to the literature review (Chapter 2, Section 2.14) to revisit the catalytic effects observed by other authors. The behaviours observed by McKee [321] for a variety of catalysts were broadly classified as:

1. General erosion in all crystallographic directions (e.g. Pb)
2. Channelling: (i) In preferred directions (e.g. V)
   (ii) Irregular (e.g. Cu, Cd)
3. Etch pit forming: (i) Hexagonal, zig-zag pits (e.g. Fe)
   (ii) Irregular (e.g. Mn, Ag)

The categories suggested by Baker [322], on the other hand, were non-wetting, wetting channelling and edge recession caused by spreading. These are summarised in Figure 6-14.

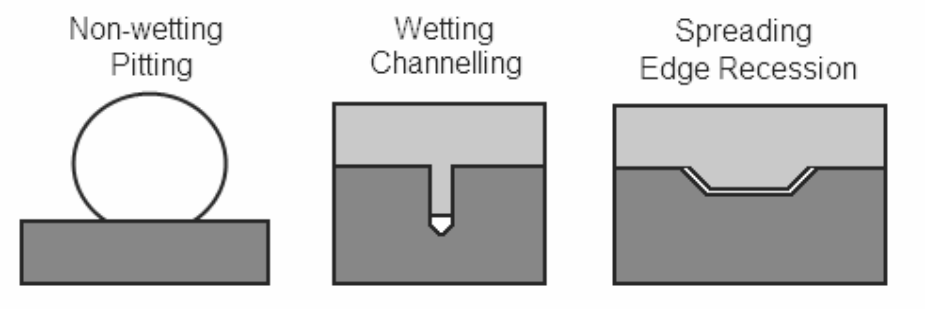

Figure 6-14: Catalyst modes of attack

Starting with the behaviours of Baker, one of these was rarely observed in RFL graphite, namely the wetting channelling behaviour. Usually, this behaviour is coupled with a faceted channel tip, as shown in Figure 6-15: the observed particle appears to have 120º angles between the faces as expected. In the subsequent images contrast and brightness are purposefully incorrect to allow easy visual identification of the catalyst and accentuation of the surface effects.

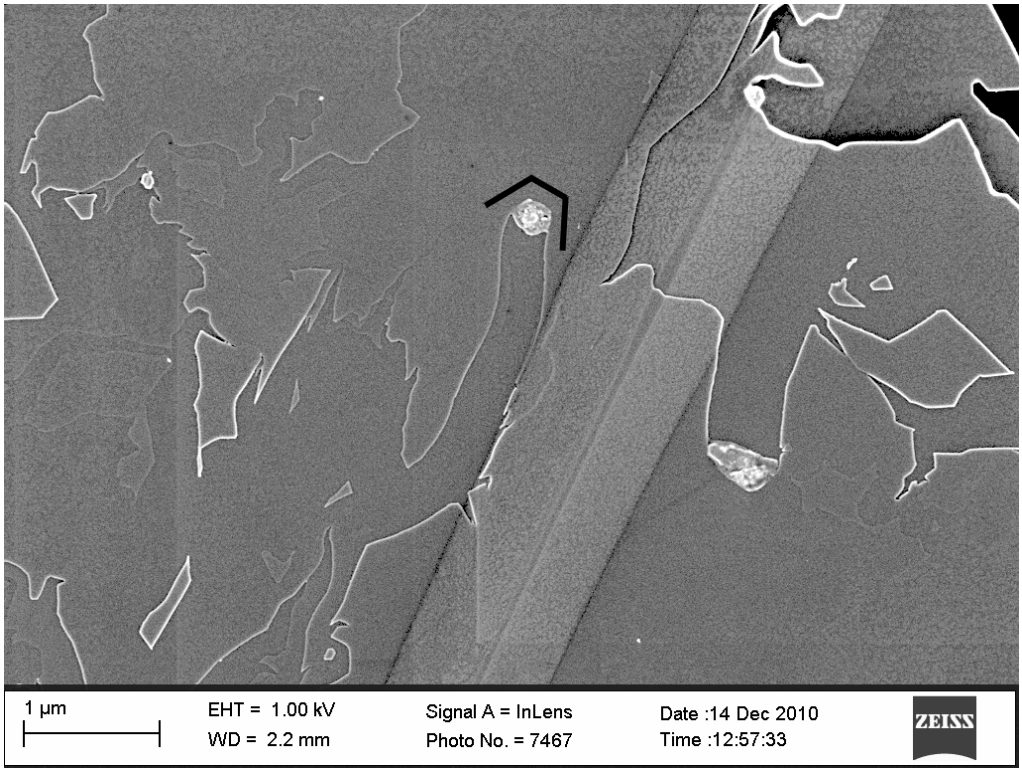

Figure 6-15: Wetting channelling catalyst (40 000x magnification)

In some cases small, round particles are observed and it is difficult to tell whether these are liquid during reaction, since they don't appear faceted. An example is presented in Figure 6-16. It is unclear whether these catalysts can be classified as wetting channelling.

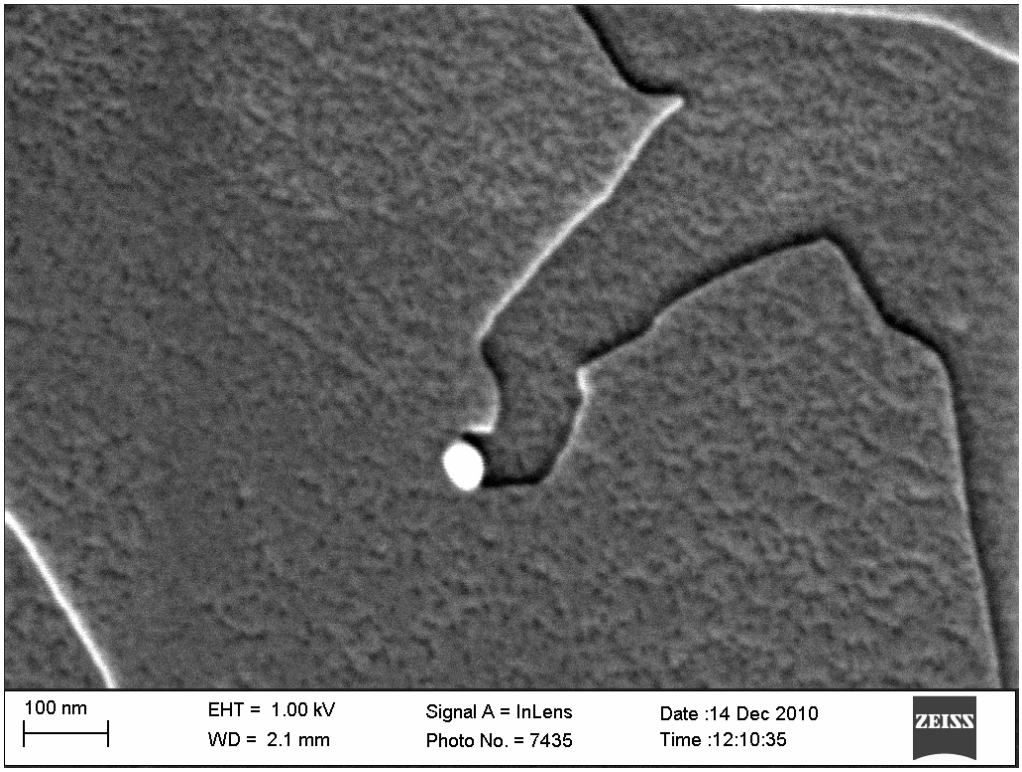

Figure 6-16: Small catalyst particle (250 000x magnification)

Outright edge recession due to spreading was not observed at all. However, a peculiar mixture between spreading and wetting channelling was observed, as shown in Figure 6-17.

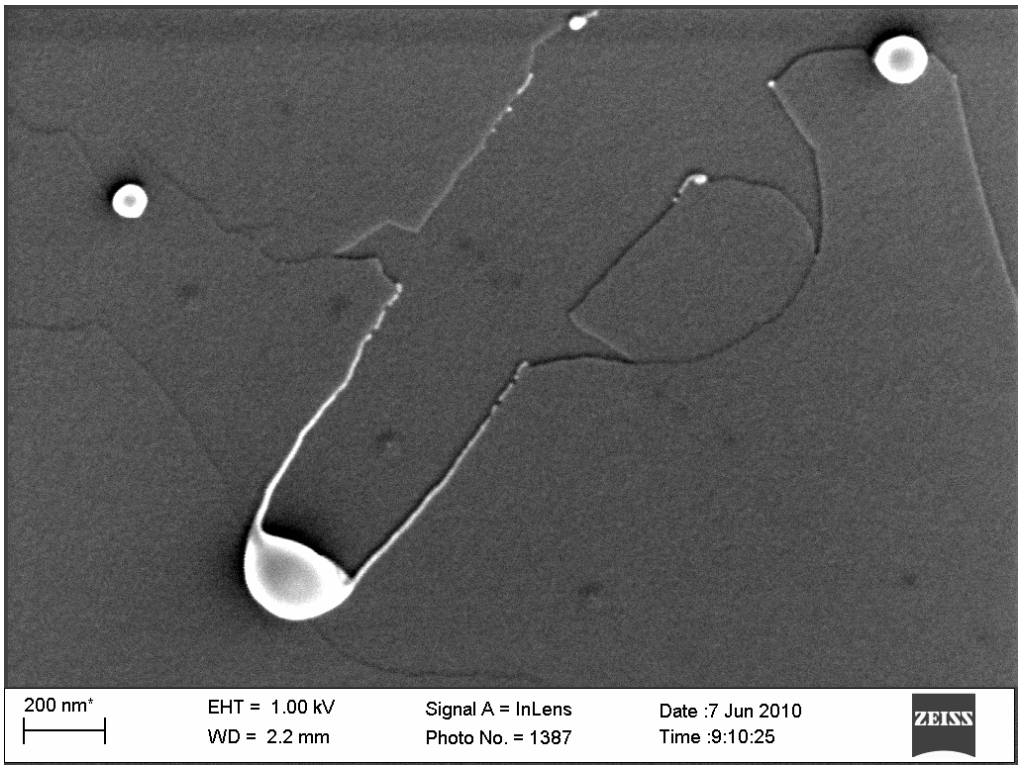

Figure 6-17: Spreading channelling behaviour (120 000x magnification)

In this case the particle was clearly molten during the oxidation, but the channel tip does not appear faceted. Furthermore, the particle is clearly spreading along the edge as the channel proceeds, leaving behind some catalytic material on the channel walls. However, there appears to be negligible widening of the channel after the catalyst particle has moved past. This would indicate that the reaction rate at the channel tip is much higher than that at the channel walls. Considering that the same catalyst is present in both areas, the difference in reaction rate is unexpected and difficult to explain.

Far more dominant are the channelling behaviours of McKee and variants thereof, i.e. erratic channelling and channelling along preferred directions. This is not unexpected since it seems unlikely that the samples are contaminated with pure metals, which formed the basis of Baker's investigation. A variety of channelling behaviours along preferred directions and along random paths are observed. At first glance it appears that small, spherical particles show a tendency towards channelling along preferred directions, as indicated by Figure 6-18 to Figure 6-20.

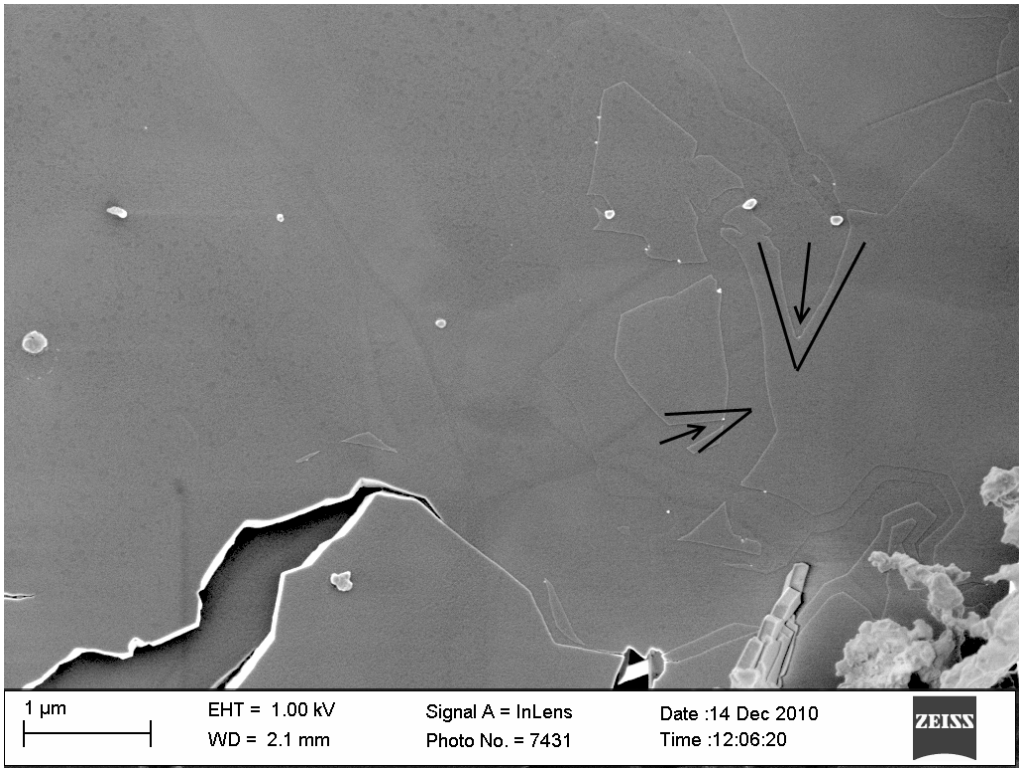

Figure 6-18: Triangular channelling (38 000x magnification)

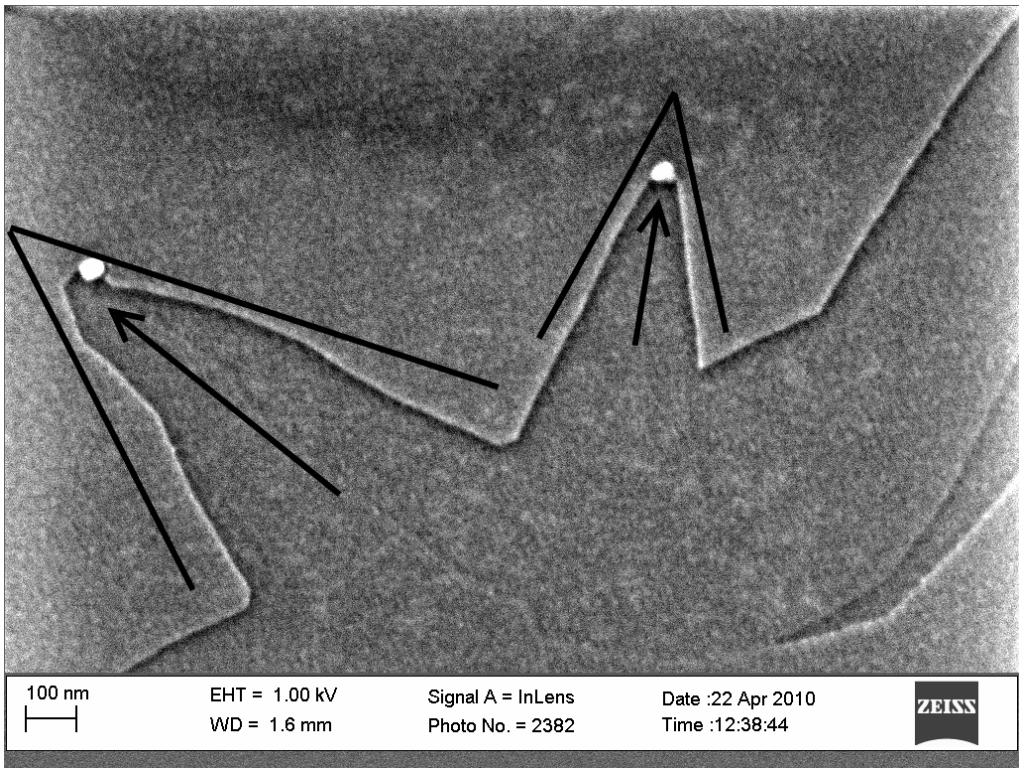

Figure 6-19: Triangular channelling (150 000x magnification)

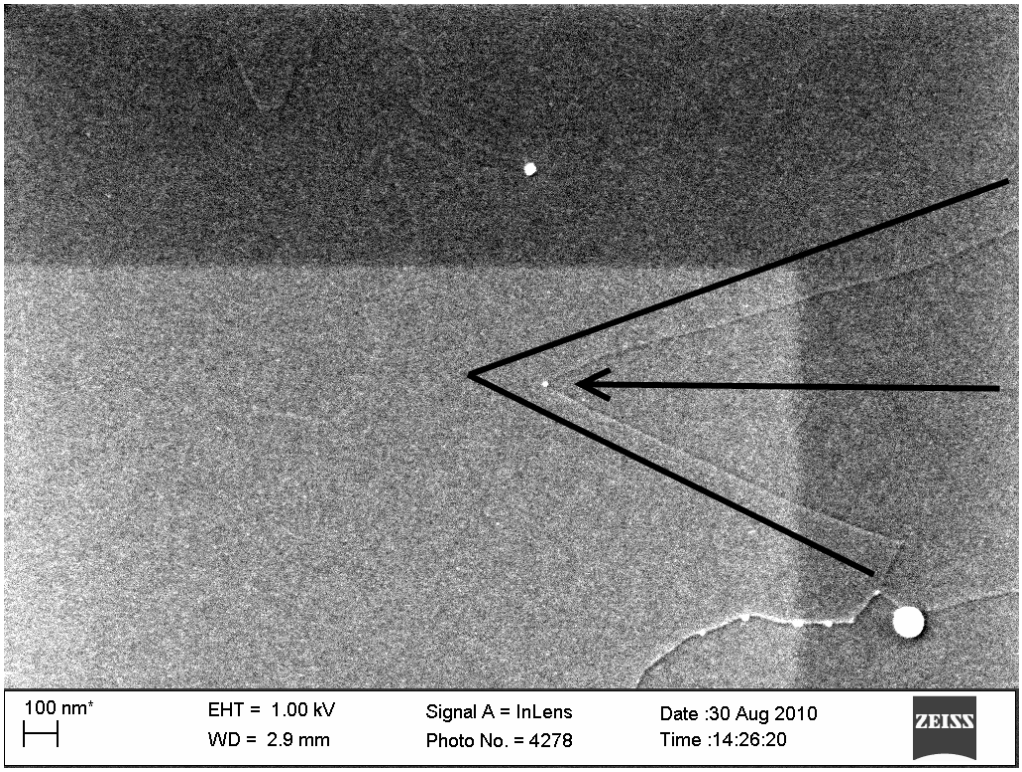

Figure 6-20: Triangular channelling (100 000x magnification)

The particles seem to consistently form roughly triangular channels in the graphite. This would indicate that the catalysed and uncatalysed oxidation rates are comparable. In this case the ratio of the channel half-width at the triangular base to the distance from the base to the tip may be used to estimate the ratio of these reaction rates. This was done for the particle shown in Figure 6-20, which indicates a catalysed to uncatalysed reaction ratio of 2.5. However, on further investigation it was found that some small particles trace erratic channels, e.g. in Figure 6-21.

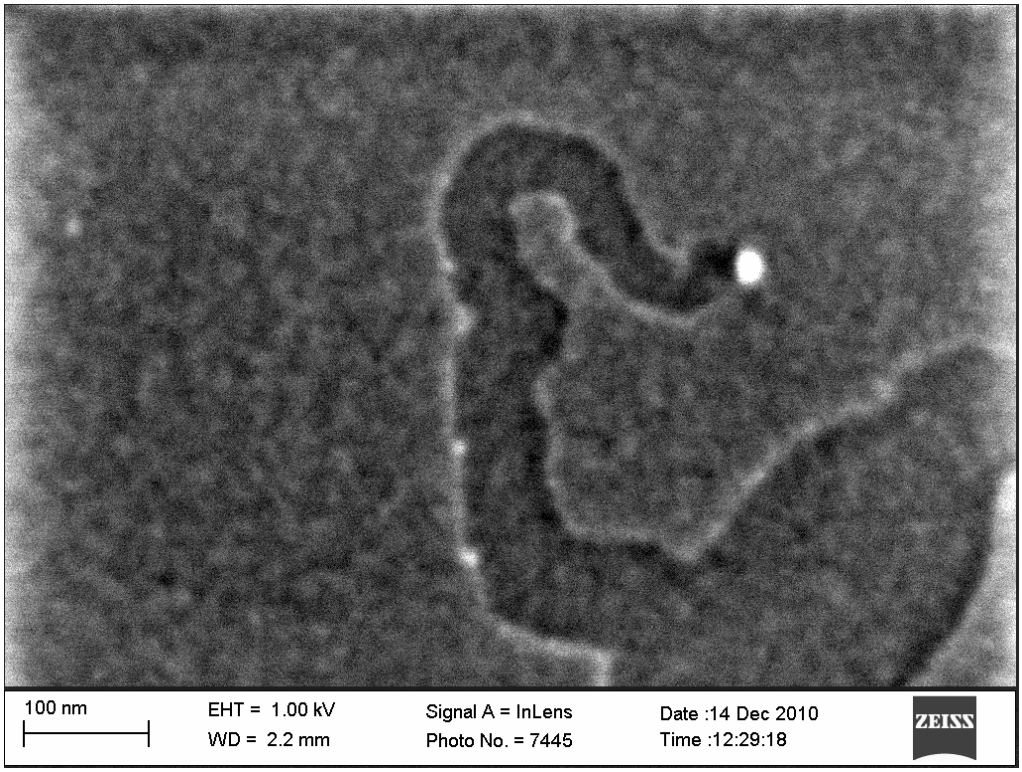

Figure 6-21: Small particle erratic channelling (370 000x magnification)

Small particles also frequently execute turns along preferred crystallographic directions, maintaining angles of 120º between subsequent channelling directions, as illustrated in Figure 6-22 and Figure 6-23. This is consistent with the internal angles of a hexagon and channelling along these preferred crystallographic directions. Based on the literature, these turns are thought to occur at lattice defects or vacancies.

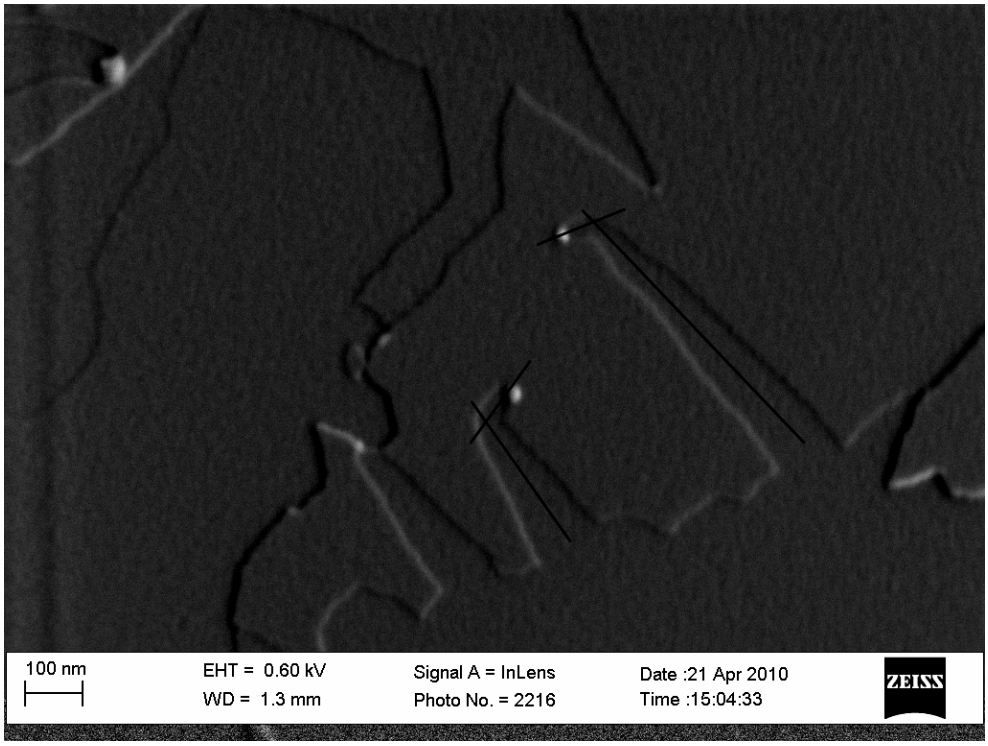

Figure 6-22: Channel turns along crystallographic directions (125 000x magnification)

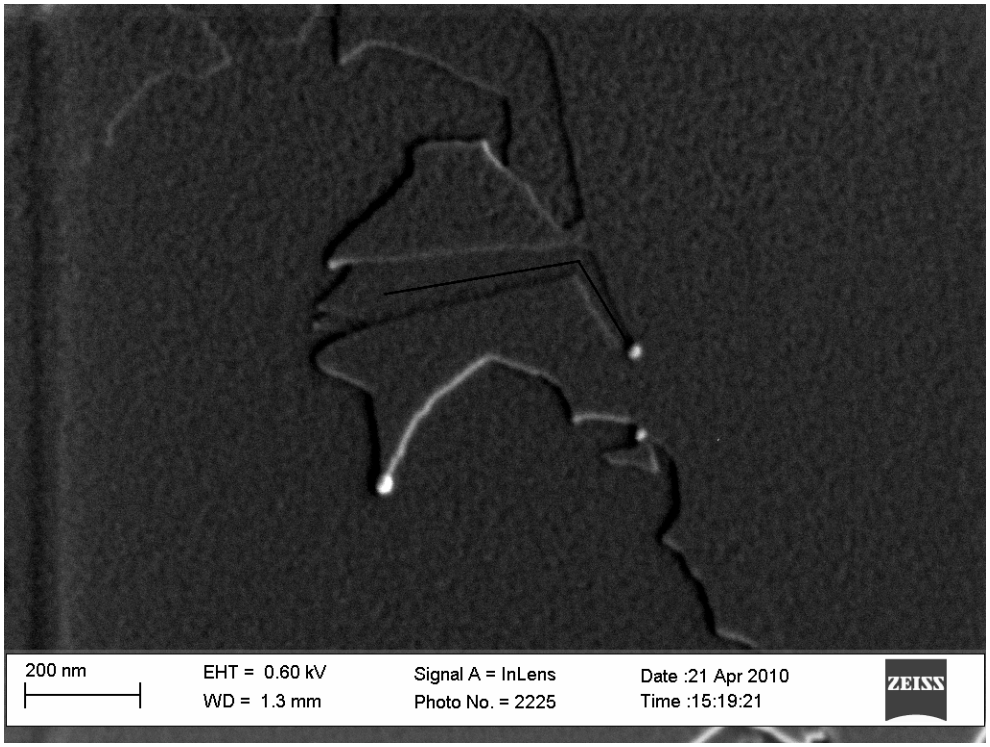

Figure 6-23: Channel turns along crystallographic directions (220 000x magnification)

In some cases a particle may execute several of these turns in rapid succession, possibly due to regions of higher defect concentrations. This leads to the appearance of an apparently erratic channel, despite the fact that the particle was still moving along preferred directions, e.g. in Figure 6-24.

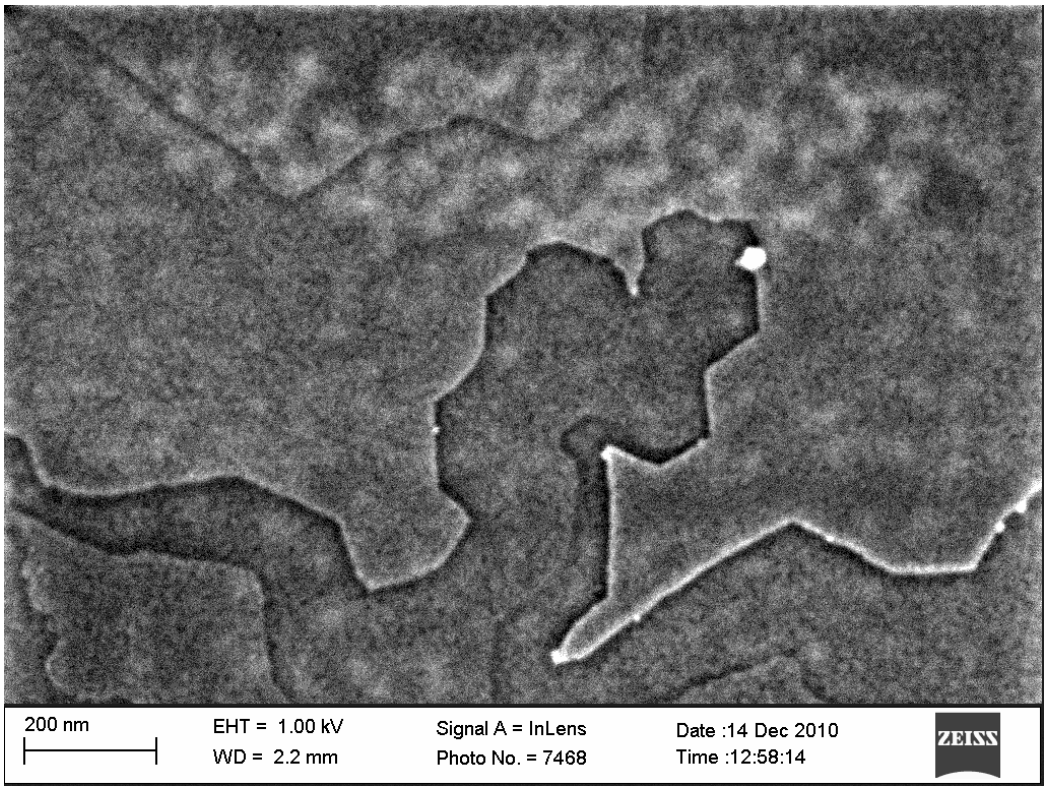

Figure 6-24: Multiple channel turns along crystallographic directions (190 000x magnification)

Thus it is not possible to link the behaviour of small spherical particles exclusively to either erratic channelling or channelling along preferred crystallographic directions. Furthermore, these spherical particles appear to undergo agglomeration and deactivation, as can be seen in Figure 6-25. The smaller particles that are still active are indicated with arrows, while the larger particle, which appears to have stalled, is indicated by the circle.

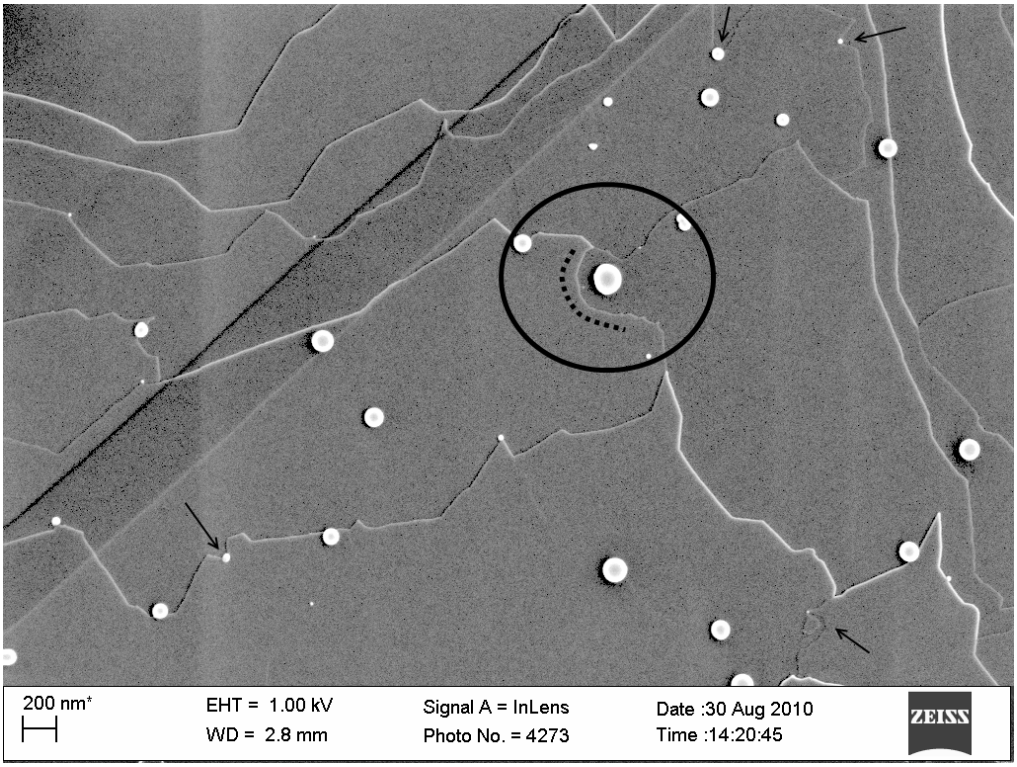

Figure 6-25: Particle agglomeration and deactivation (50 000x magnification)

A circular ring of oxidation is spreading out from the particle, as indicated by the dashed curve. This indicates that the particle was propagating a channel in the graphite but that at some point it stopped moving and the channel tip proceeded to grow under uncatalysed oxidation. This would indicate that the particle was not wetting the channel tip, as it would have adhered to the free edge. However, the particles generally appear to be perfectly spherical, which seems to indicate they were in a liquid state at the oxidation temperature.

It is possible to postulate the presence of the "action at a distance" mechanism observed by Yang and Wong [300], whereby the catalyst particle acts as a dissociation centre and there is oxygen spill-over. This causes rapid edge recession at some distance from the particle. However, the presence of several, similarly sized, stationary particles with no visible oxidation effects would seem to indicate that this is not the case.

By far the most commonly observed behaviour is random, erratic channelling caused by large, irregularly shaped particles, as shown in Figure 6-26 to Figure 6-30.

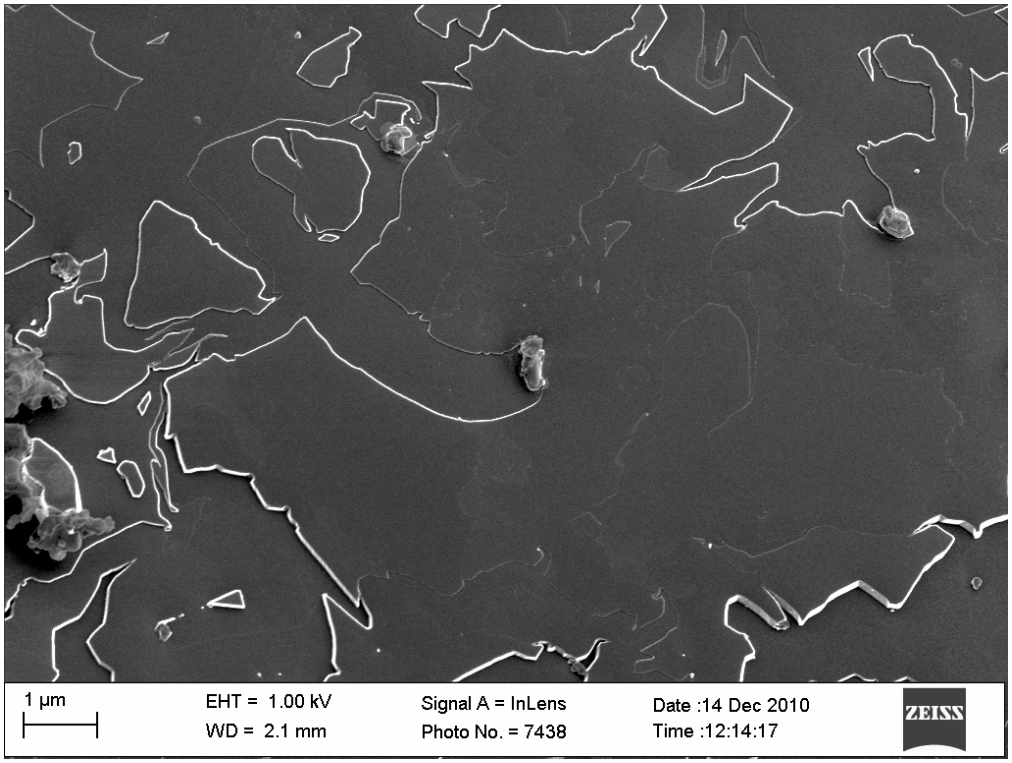

Figure 6-26: Random erratic channelling 1 (45 000x magnification)

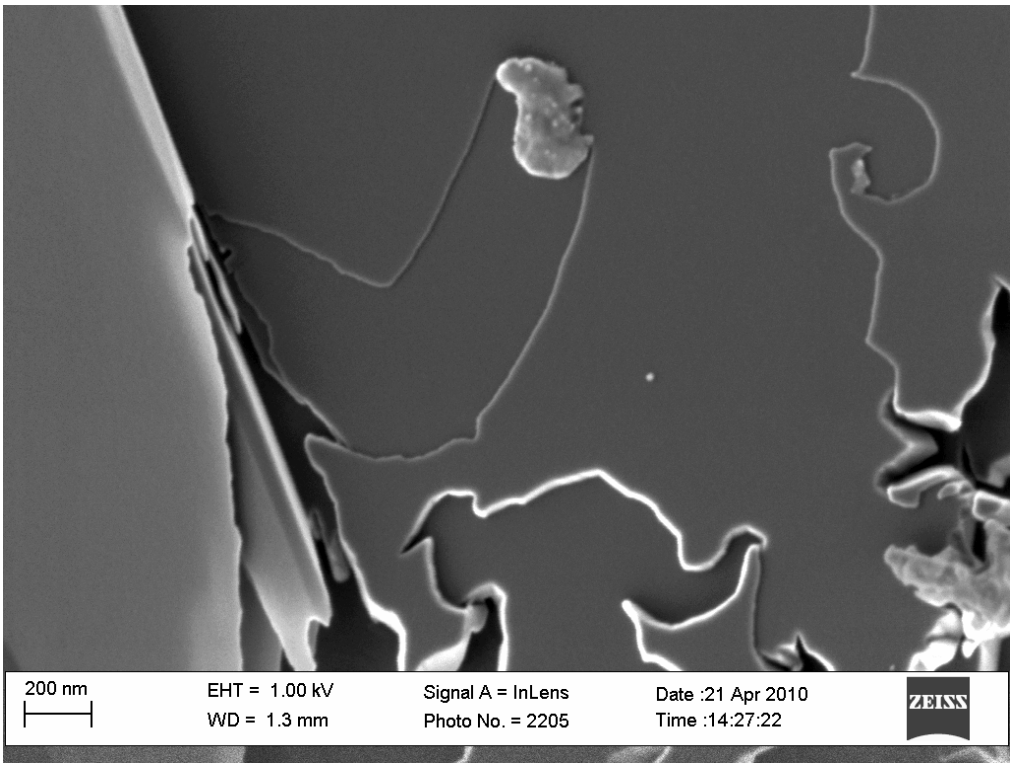

Figure 6-27: Random erratic channelling 2 (100 000x magnification)

Figure 6-28: Random erratic channelling 3 (101 000x magnification)

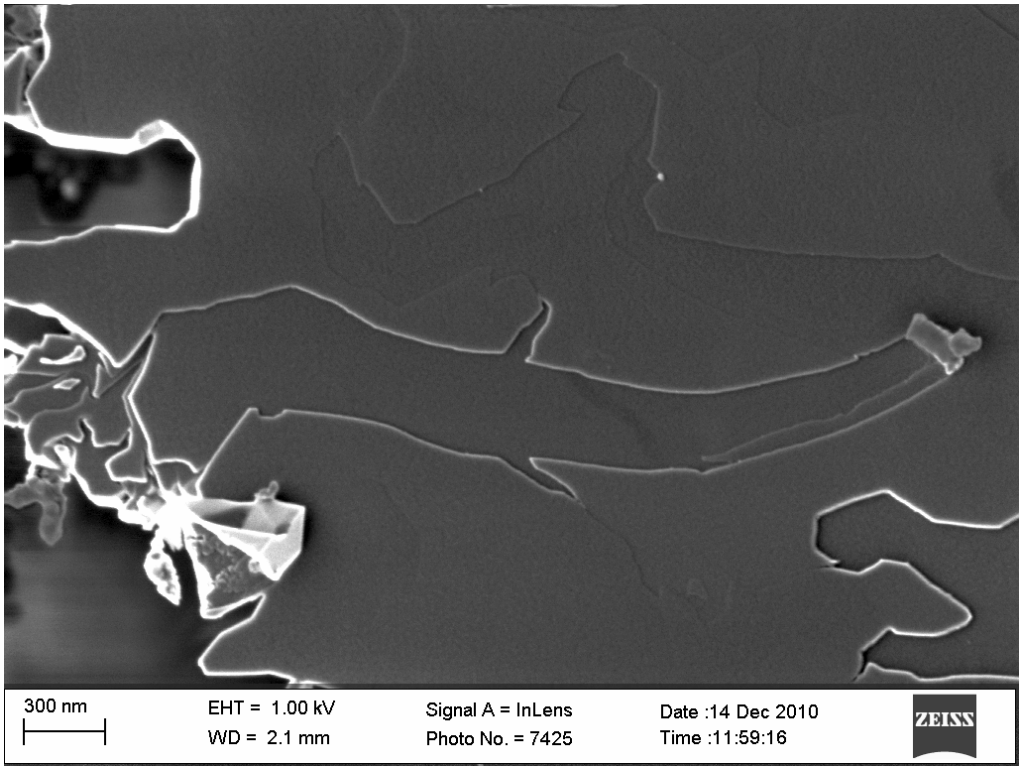

Figure 6-29: Random erratic channelling 4 (80 000x magnification)

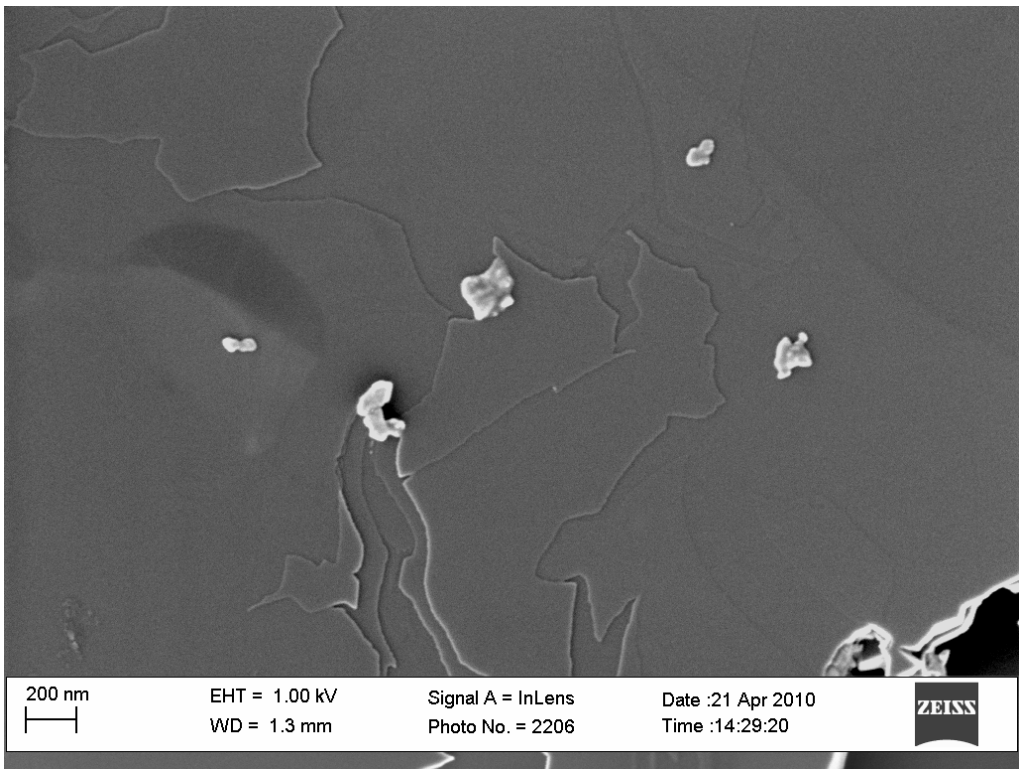

Figure 6-30: Random erratic channelling 5 (75 000x magnification)

The shape of these particles would seem to indicate that they are solid at reaction temperature and maintain their shape throughout. The movement of these particles can be very complex as the surface is highly irregular. This is in accordance with the observations made by Tomita and Tamai [310]. The movement is governed by the postulate that the particle is at all times trying to maintain the largest contact area with the graphite plane. However, surface irregularities will cause random variations in the contact points of the particle with the surface. Oxidation at these points will accelerate the movement of the particle randomly in a variety of directions, resulting in the erratic channels observed and continuous three-dimensional shifting, turning and rotation of the particle.

The last two images, namely Figure 6-29 and Figure 6-30, illustrate extreme cases of this random movement and rotation of the particle. The particles are found to be capable of tracing channels in two discrete steps in the graphite. This leads to two randomly shaped furrows in the graphite as the particle passes through. Under no circumstances was it found that these particles move along preferred crystallographic directions. Thus these large, irregularly

shaped, particles appear to consistently trace erratic channels through the graphite due to the fact that they are solids at the oxidation temperature.

It seems plausible that the random channelling behaviour observed previously for small, apparently spherical, particles is caused by the fact that they are in fact not spherical but also irregular solids, such as the particles just discussed. However, their features may simply be too regular or too small to discern. An example of a very small particle tracing an erratic channel is shown in Figure 6-31. In this case the erratic shape is easily distinguishable. It is interesting to note that despite the erratic nature of the channel, the particle still seems to execute a 120º turn. Thus although it seems to be moving along a preferred direction, the resulting channel is erratic due to the erratic shape of the particle.

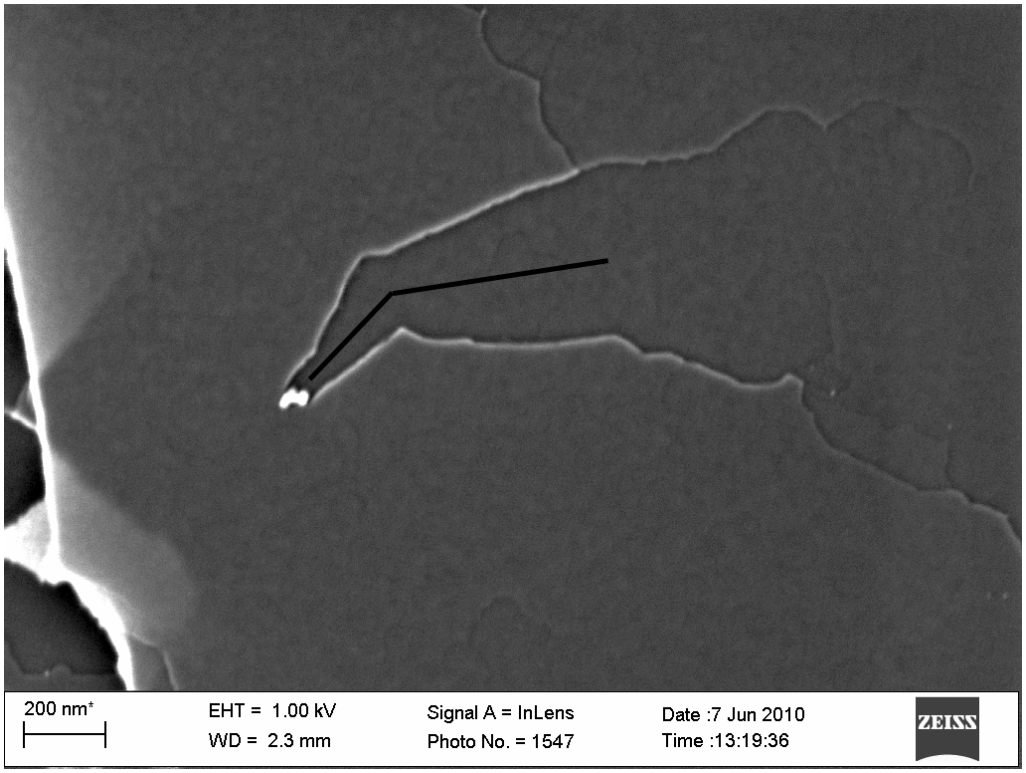

Figure 6-31: Random erratic channelling of small particle (120 000x magnification)

The extremely erratic, almost fractal-like, edge of the oxidised RFL graphite is clearly a result of particles tracing randomly orientated channels into the flake. These channels criss-cross each other as the particles move. This also

accounts for the fairly limited penetration into the samples since the more random their movement, the more likely they are to remain along the graphite edge. This roughening effect is clearly demonstrated by Figure 6-32 and Figure 6-33.

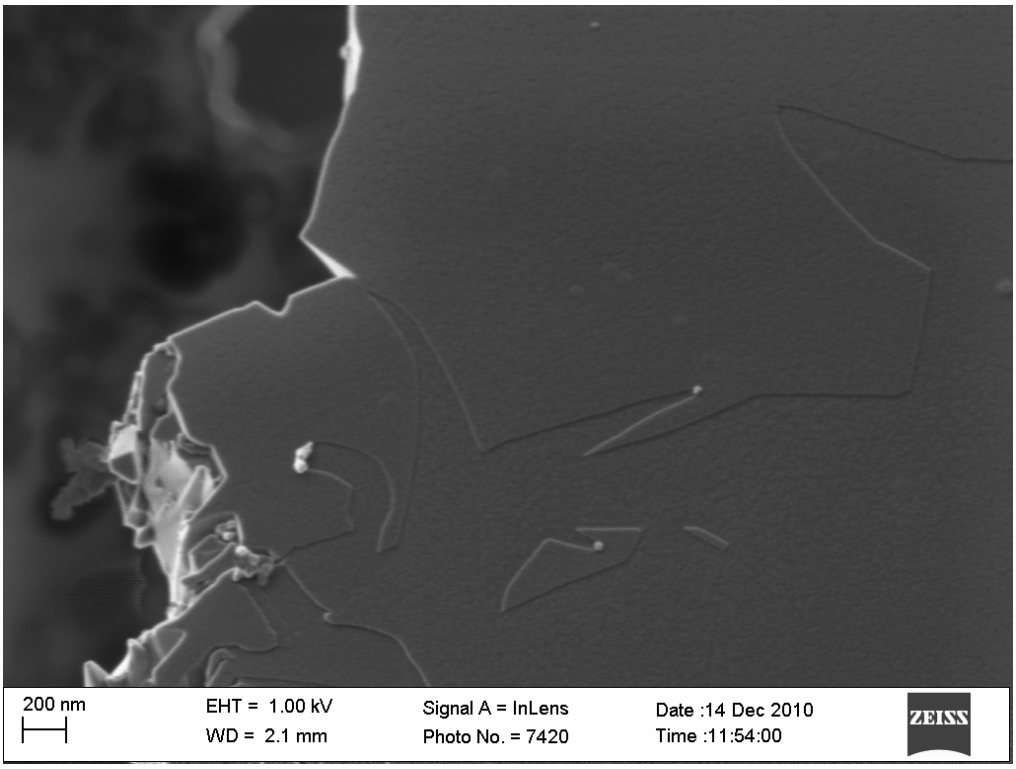

Figure 6-32: Fractal-like edge roughening 1 (65 000x magnification)

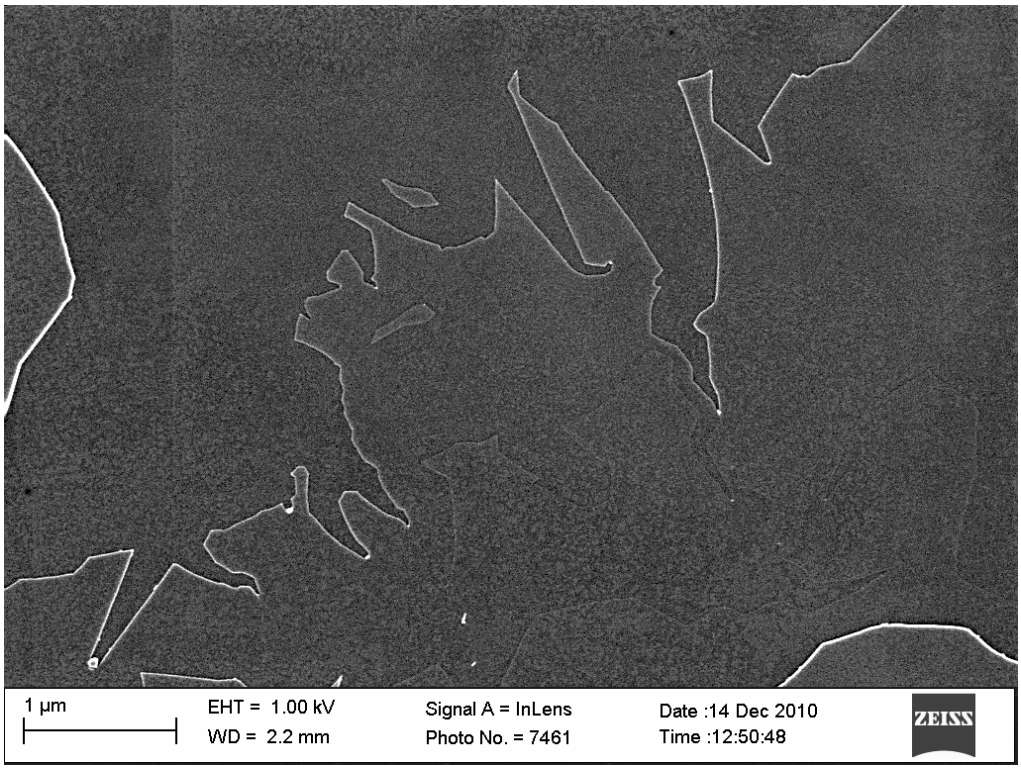

Figure 6-33: Fractal-like edge roughening 2 (45 000x magnification)

It is clear that a very wide variety of channelling behaviours can be distinguished. These behaviours do not all fall into clearly distinguishable categories and in some cases particles seem to exhibit combinations of the typical behaviours. This is not unexpected since the RFL graphite is naturally mined and is bound to contain a wide variety of impurities with arbitrarily varying characteristics. The partially purified RFL graphite, on the other hand, exhibits a far more limited range of channelling behaviours.

At low and intermediate conversions, the partially purified materials exhibit hardly any catalytic behaviour. However, at high conversions, the appearance of catalytic channels is clearly evident. This would indicate that the catalyst is trapped inside the particles and only released once a large part of the material has been oxidised away. At first glance in Figure 6-34 the flakes do not appear to have appreciable roughening or the fine edge structures found in the flakes considered earlier.

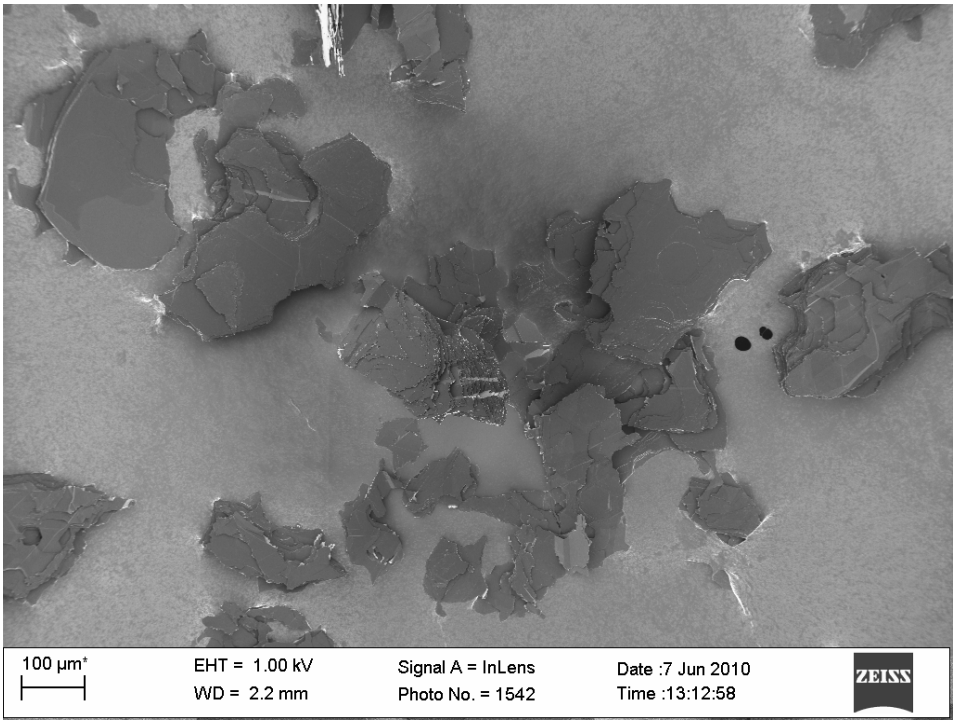

Figure 6-34: Partially purified flakes (200x magnification)

However, when the flakes are examined more closely, the edges do appear roughened, as can be seen in Figure 6-35.

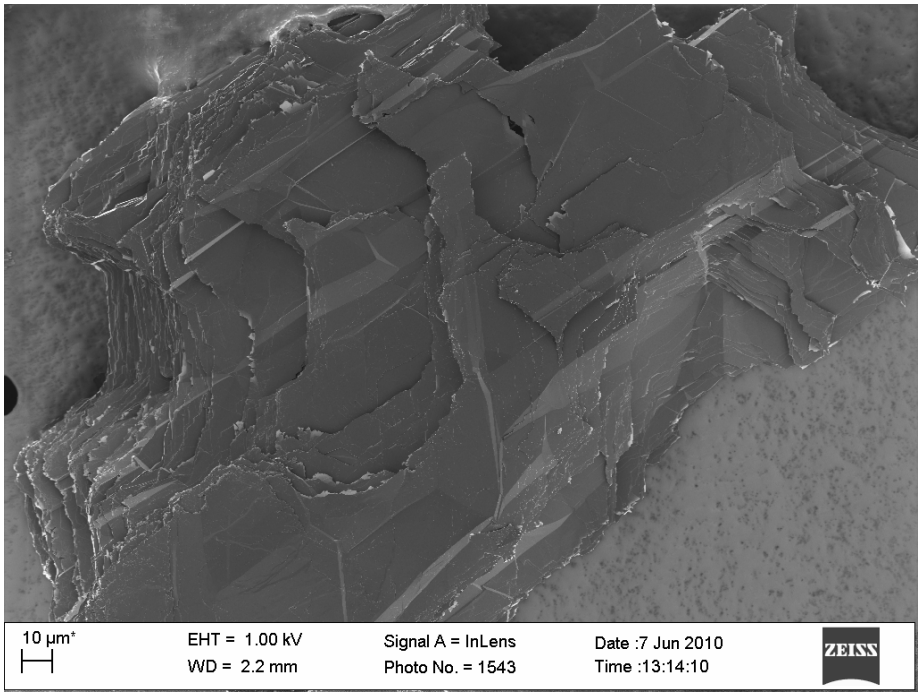

Figure 6-35: Partially purified flake (1 000x magnification)

However, upon further magnification the roughness is seen to consist of flat, regular, triangular structures with a clear 120º angle. This is very similar to the edge structures observed for the fully purified material. The observed roughening is therefore not caused by catalytic activity.

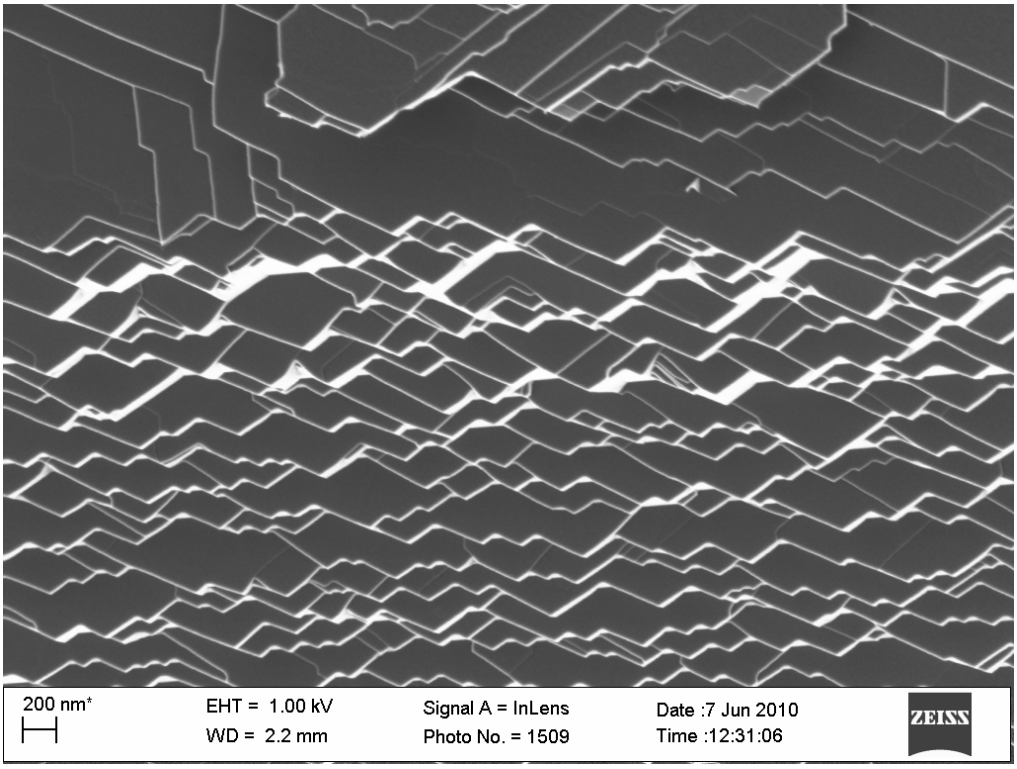

Figure 6-36: Partially purified flake edge (50 000x magnification)

Only on a few discrete flakes is channelling activity evident. As can be seen from Figure 6-37, individual catalyst particles and channels are readily discernible. Channel penetration into the flake is significant, cutting easily identifiable, repeatable, triangular channels into the flake. This is in stark contrast to the highly erratic, chaotic edges encountered in the as-received material.

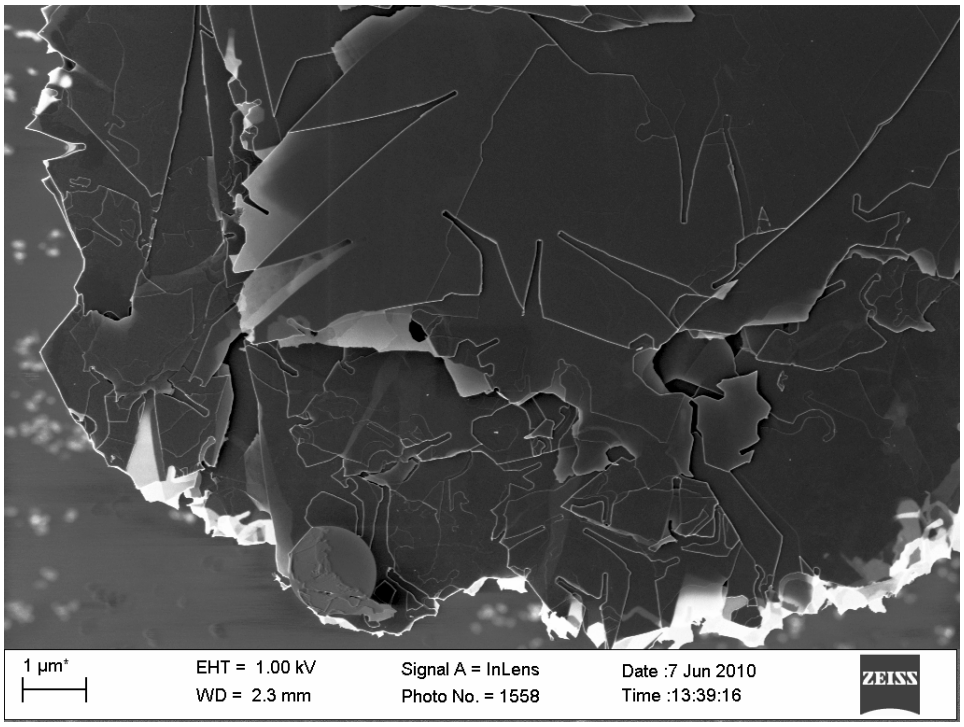

Figure 6-37: Partially purified flake catalyst activity (20 000x magnification)

Closer examination of the channels reveals a funnel-like appearance, as shown in Figure 6-38.

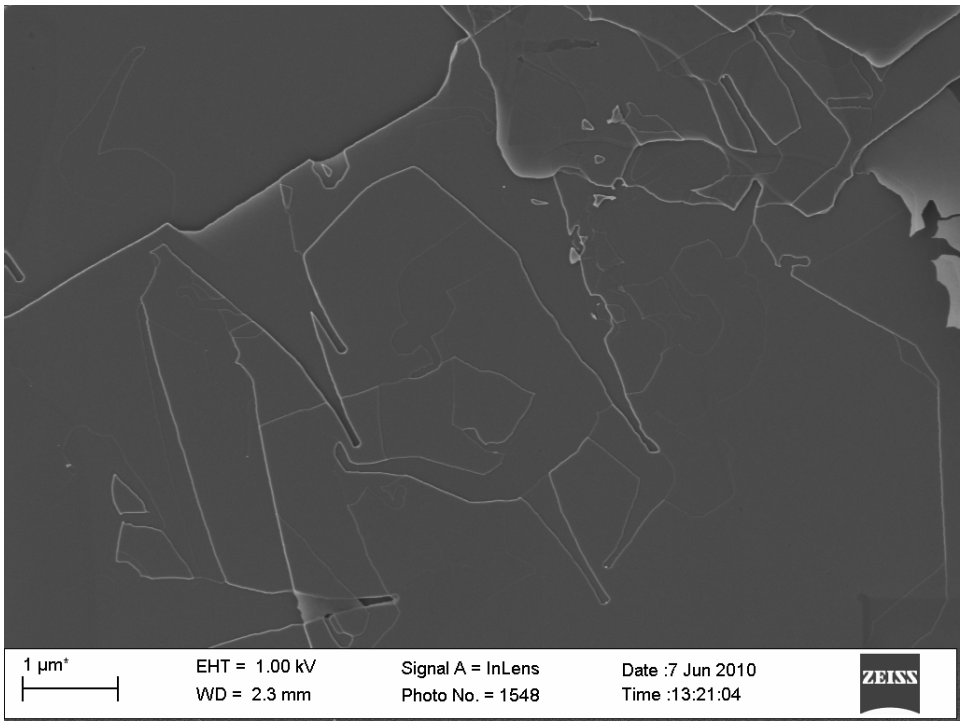

Figure 6-38: Funnel-shaped channels (30 000x magnification)

The reason for this behaviour is two-fold. Firstly, the catalytic channelling rate is significantly faster than the uncatalysed reaction rate. This leads to the formation of straight channel tips with negligible uncatalysed oxidation, as typified by the channels shown in Figure 6-39.

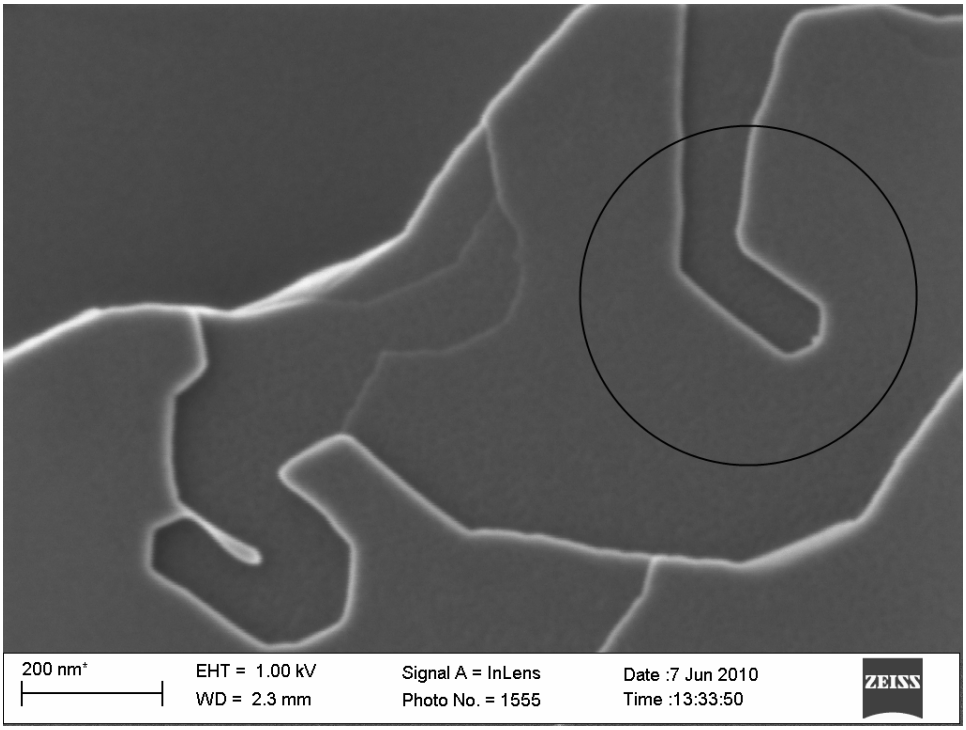

Figure 6-39: Straight channel tips (220 000x magnification)

To understand the second effect that contributes to the channels' characteristic shape it is first necessary to examine the crystallographic orientation present at the graphite edges. As mentioned in the theoretical background (Chapter 2), graphite twins usually present in pairs, leading to the formation of so-called “twin lamellae” or “twin bands”. These bands represent a rotation of 20º along the basal plane, followed by another 20º rotation in the opposite direction to restore the original orientation. These small inclines are readily discernible from the topographic nature of the SEM imaging and can be easily identified, as shown in Figure 6-40 and Figure 6-41. In addition, as also discussed previously, if an oxidation pit is in the vicinity of the twin, the edge orientation of the pit can be readily identified as armchair if the pit is parallel to the twin, or zig-zag if it is perpendicular. A variety of twins are visible as indicated by the dashed lines.

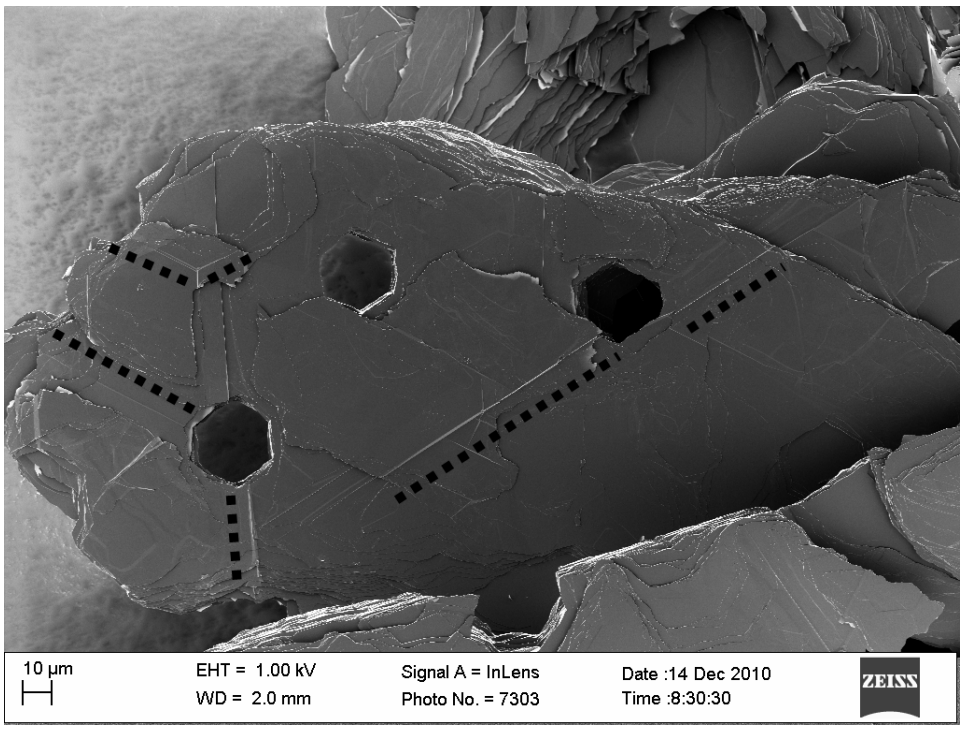

Figure 6-40: Edge orientation from twinning example 1 (900x magnification)

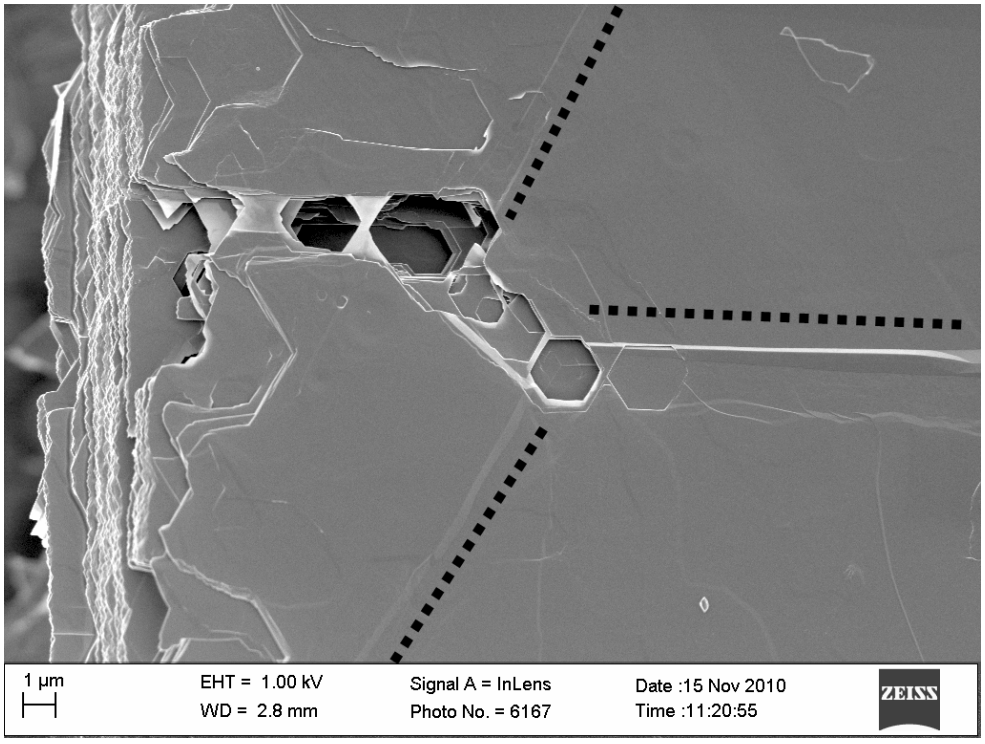

Figure 6-41: Edge orientation from twinning example 1 (10 000x magnification)

Furthermore, it is clear that the pit edges are orientated parallel to the twins and hence the edge configuration is armchair. This is consistent with the work of Thomas [10], which indicated that below 900 ºC the armchair configuration should dominate during uncatalysed oxidation due to the slightly higher reactivity of the zig-zag edge sites. By comparing the pit edges with the formations found at the flake edges, as shown in Figure 6-42, it may be more generally asserted that the oxidation along the entire flake edge is proceeding along the armchair face.

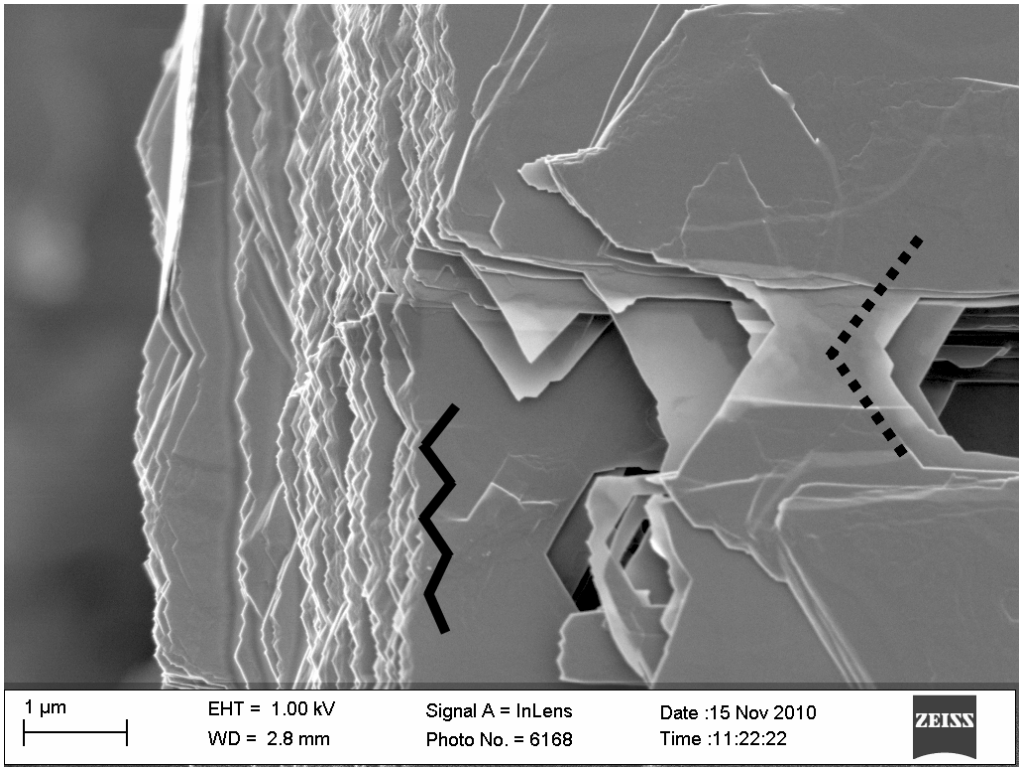

Figure 6-42: Flake edge orientation (30 000x magnification)

However, if the direction of the catalyst channels relative to the flake edge is examined, as in Figure 6-43, the channels are found to be exclusively oriented perpendicular to the edge. This indicates that the channelling is occurring exclusively along the zig-zag edge.

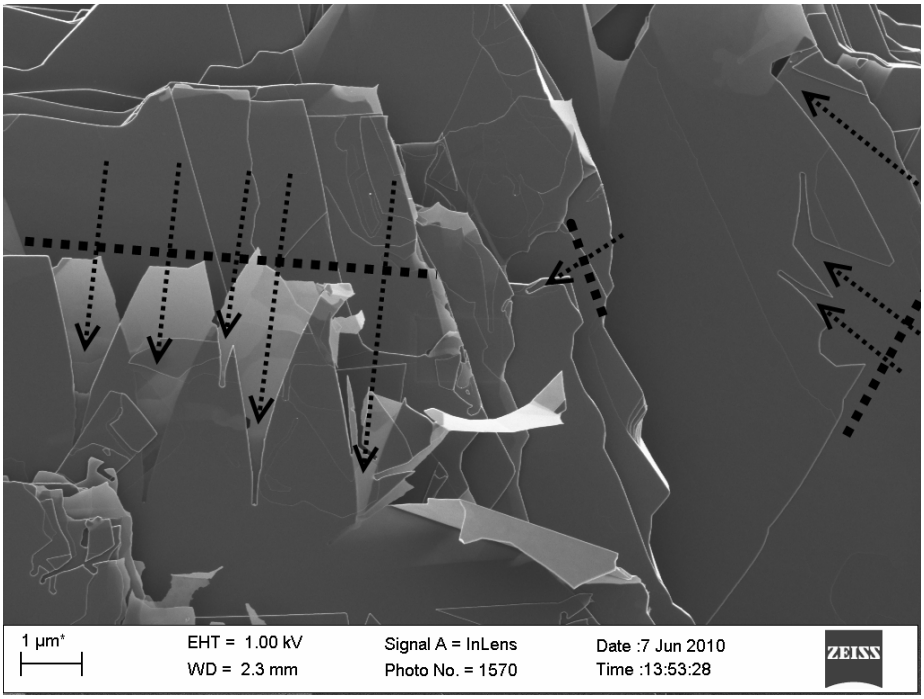

Figure 6-43: Channel-to-flake-edge orientation (20 000x magnification)

When a catalytic channel that has progressed significantly into the flake is examined, the edge orientation is found to change, as in Figure 6-44.

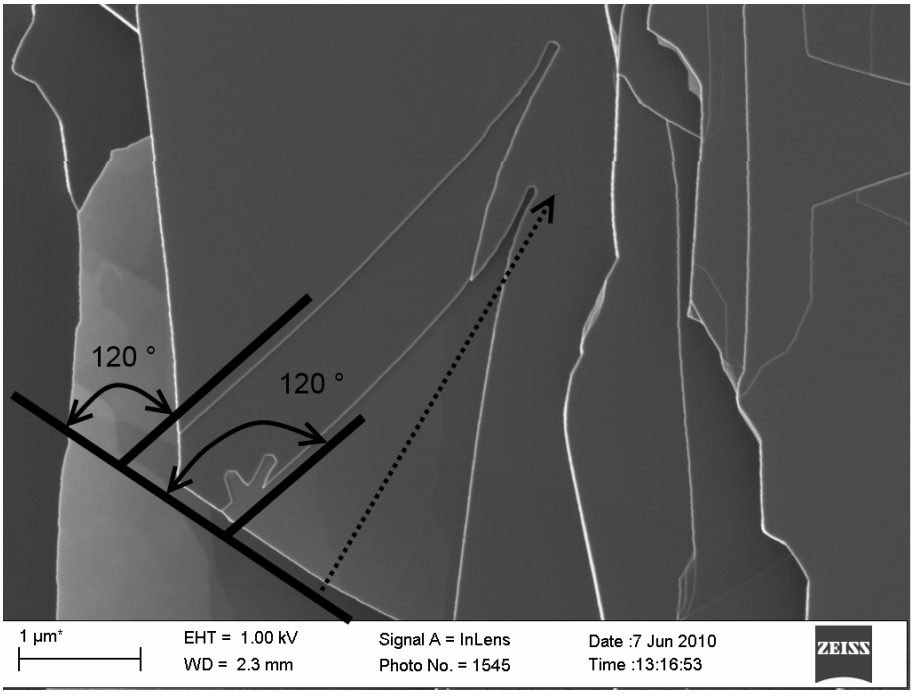

Figure 6-44: Channel-to-flake-edge orientation (40 000x magnification)

As can be seen from this figure the edge orientation, under uncatalysed oxidation, gradually undergoes a transition from an angle perpendicular to the edge, i.e. zig-zag orientation, to an angle of 120º with the edge, i.e. armchair orientation. Thus the reason for the funnel-shaped behaviour is a combination of high catalyst reactivity relative to uncatalysed oxidation, and the transition of the channel edge configuration from zig-zag to armchair. If the channel tips are examined more closely, a few more interesting characteristics are revealed, as can be seen from Figure 6-45.

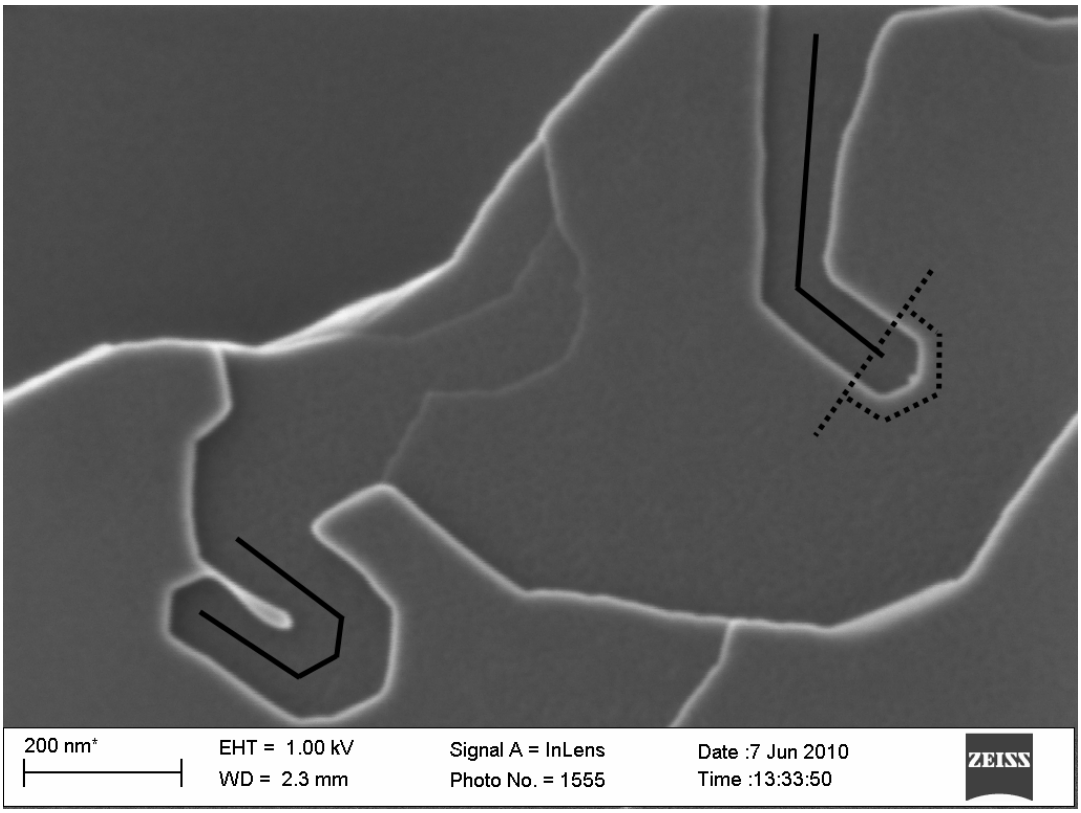

Figure 6-45: Catalyst channel tip (220 000x magnification)

Firstly, the particles readily execute 120º turns, in a similar fashion as was noted earlier for small catalytic particles on the as-received material. Secondly, the channel tip has some very distinctive features. The catalyst particle is very small, <10 nm, compared with the channel width, ~80 nm. Furthermore, the catalyst is located at the tip of a perfect half-hexagon. This behaviour is consistent across several catalyst particles. The reason for this peculiar behaviour is not clear, but this does illustrate why only a few catalyst particles

can lead to the creation of massive amounts of ASA and hence drastically affect the oxidation rates. Finally, an interesting phenomenon is found when the catalyst particles collide with an existing step in the graphite, as in Figure 6-46.

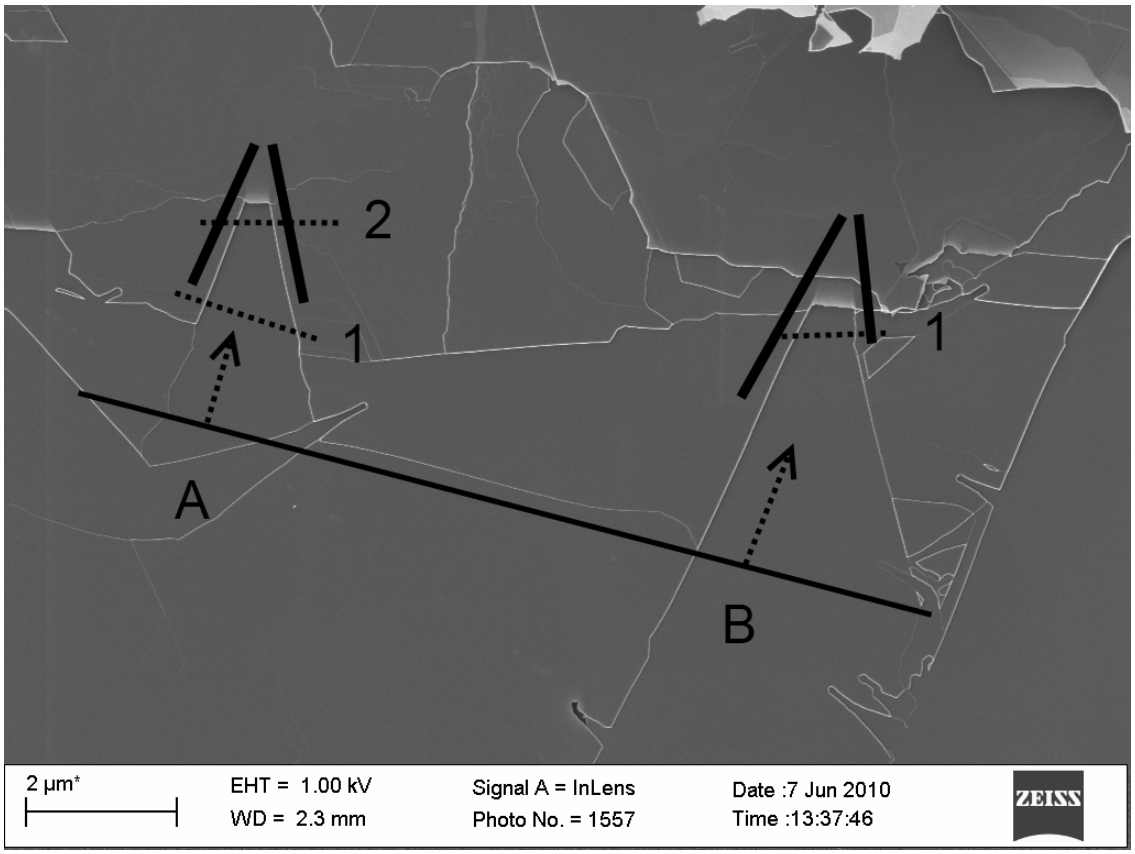

Figure 6-46: Catalyst sub-basal channelling (20 000x magnification)

The first particle, A, actually collides with two different steps, 1 and 2. During the initial collision with step 1, the particle undergoes no change and simply continues along its original trajectory. When the particle collides with step 2, it still continues along its original trajectory, as can be deduced from the constant angle of the channel wall, indicated by the thick black lines. However, in this case the particle proceeds below the basal plane and tunnels directly into the graphite. This is consistent with the behaviour of the second catalyst particle, B.

The fact that the opacity of the channel beyond this point changes from very light at the initial tunnel lip to darker as the tunnel proceeds implies that the thickness of the basal plane in this direction is increasing. This may indicate either that the particle is burrowing deeper into the graphite away from the basal

plane, or that the channel is wedge shaped. That is to say at the catalyst particle the channel is only as wide as the particle itself, while further away the channel height progressively expands up to some value close to the height of the original step.

This behaviour, coupled with the channel tip characteristics, makes it very difficult to deduce clearly the mechanism by which oxidation is proceeding. Thus despite the fact that the number of catalytic behaviours has been greatly reduced in comparison with the original material, deducing the catalytic mechanism is still problematic. It was therefore decided to take the purified material, which showed no trace of catalytic activity, and contaminate it with a single catalyst which has a distinct behaviour. Then an attempt could be made to represent this behaviour qualitatively in an effort to simulate the catalytic action and come to sensible conclusions regarding its influence on the oxidation.

For this purpose, sodium, in the form of sodium carbonate, was chosen, due to its known ability to induce highly erratic channelling effects and remain solid up to 850 ºC [296]. As mentioned in the experimental section (Chapter 3), the purified material was contaminated with sodium carbonate solution and allowed to dry, followed by oxidation. From Figure 6-47 and Figure 6-48 it is clear that the sodium is well dispersed across the particles and catalytic activity is expected to be fairly homogeneous.

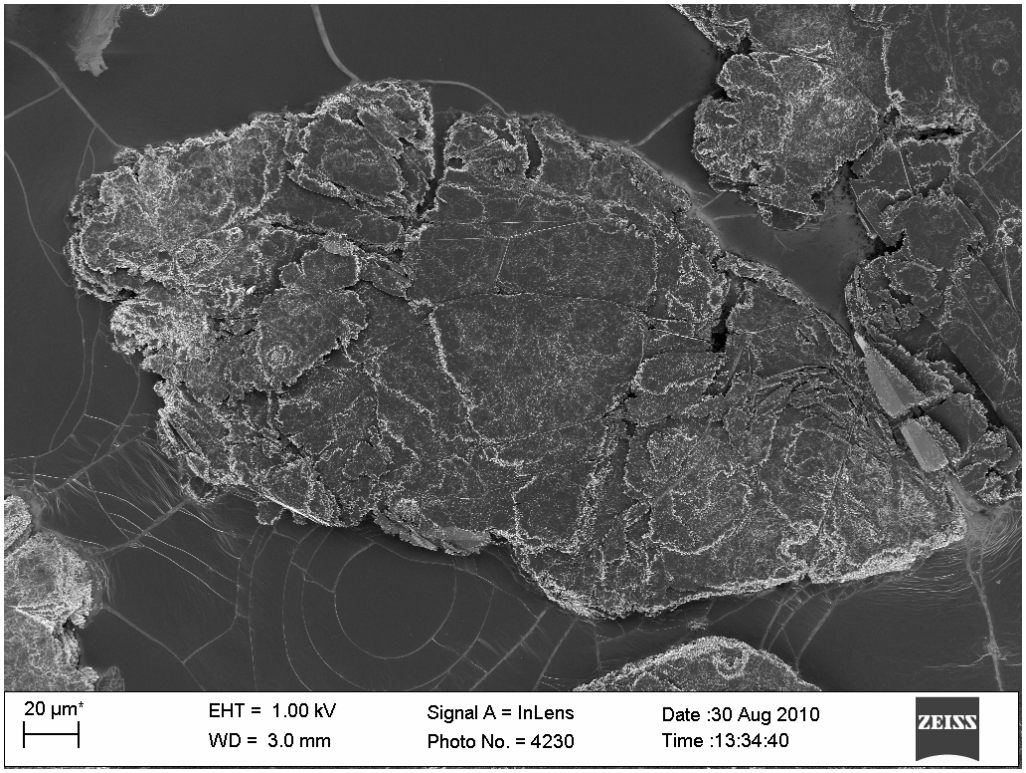

Figure 6-47: Contaminated flake 1 (800x magnification)

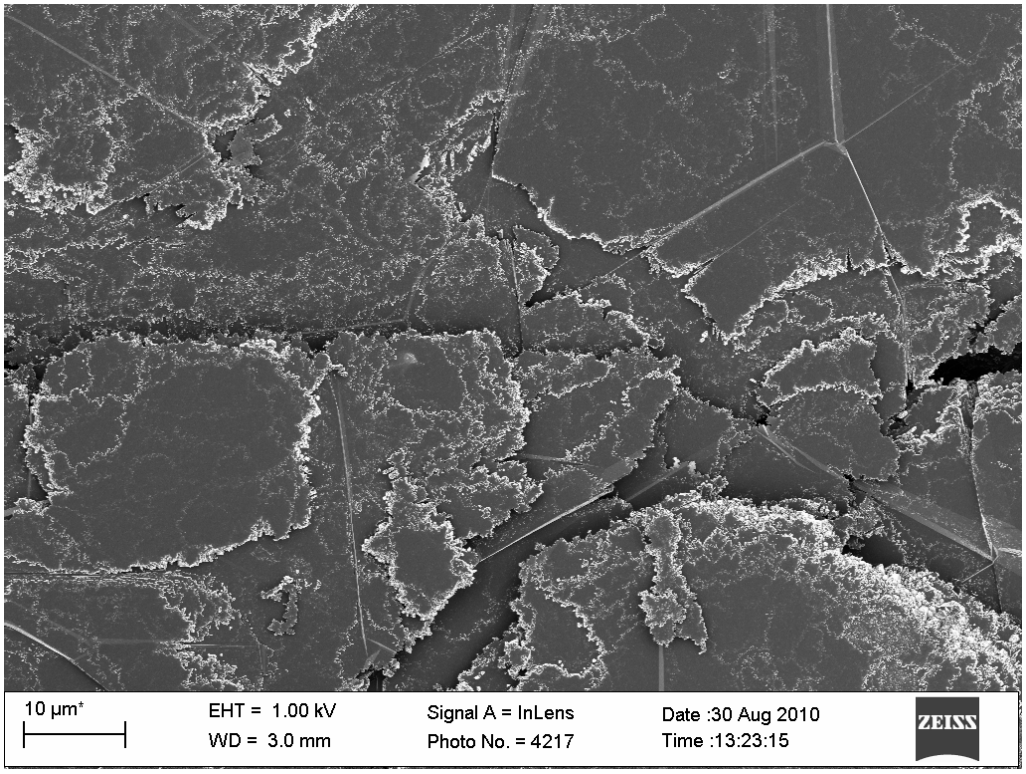

Figure 6-48: Contaminated flake 2 (3 000x magnification)

As can be seen from Figure 6-49 and Figure 6-50, the behaviour is exactly as expected. A very irregular, fine edge structure has been produced. Channel penetration into the sample is very limited and catalytic activity is localised at the edges.

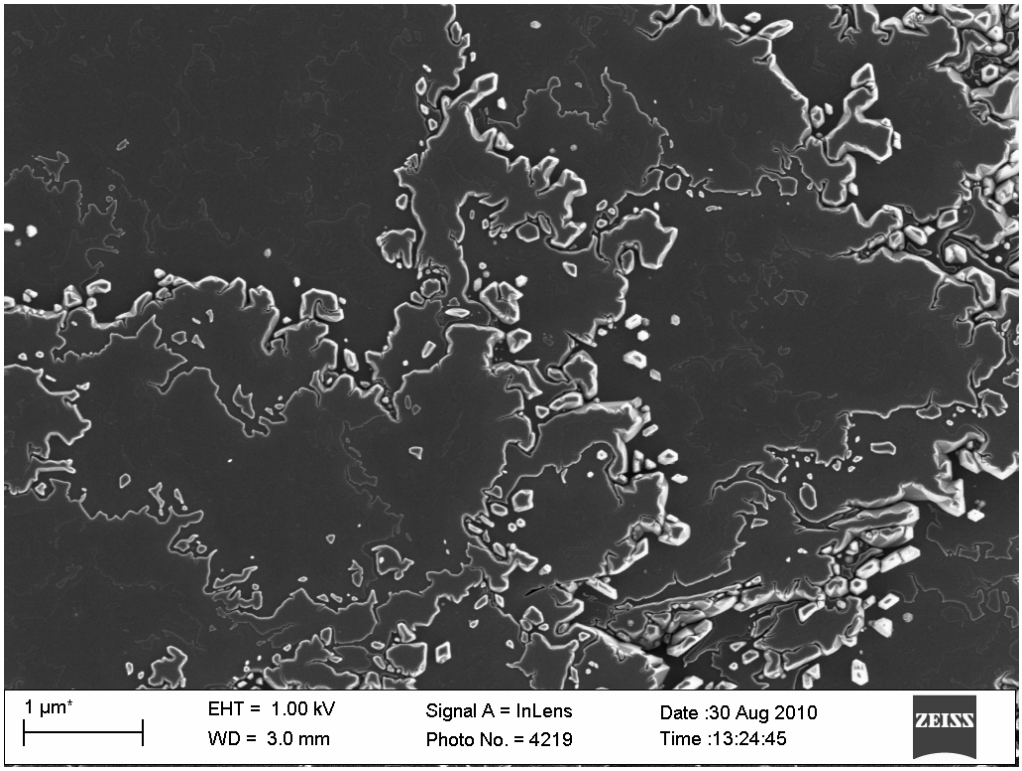

Figure 6-49: Contaminated flake-edge structure (35 000x magnification)

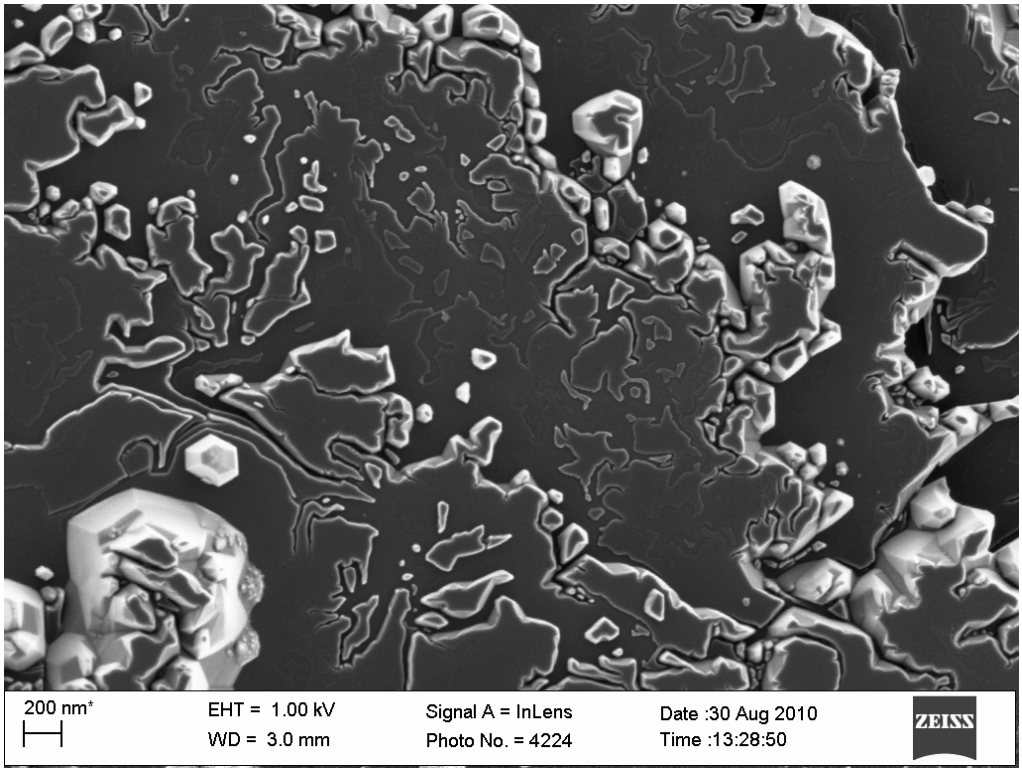

Figure 6-50: Contaminated flake-edge structure (55 000x magnification)

Individual catalyst particles are difficult to discern due to their small size, which is to be expected from the deposition method. However, in some cases they are readily visible and are seen to trace the random, erratic channels expected to underlie the observed edge structures, as shown in Figure 6-51 and Figure 6-52. The particle movements may be noted as resembling Brownian motion or a random walk, and show no preferred orientation.

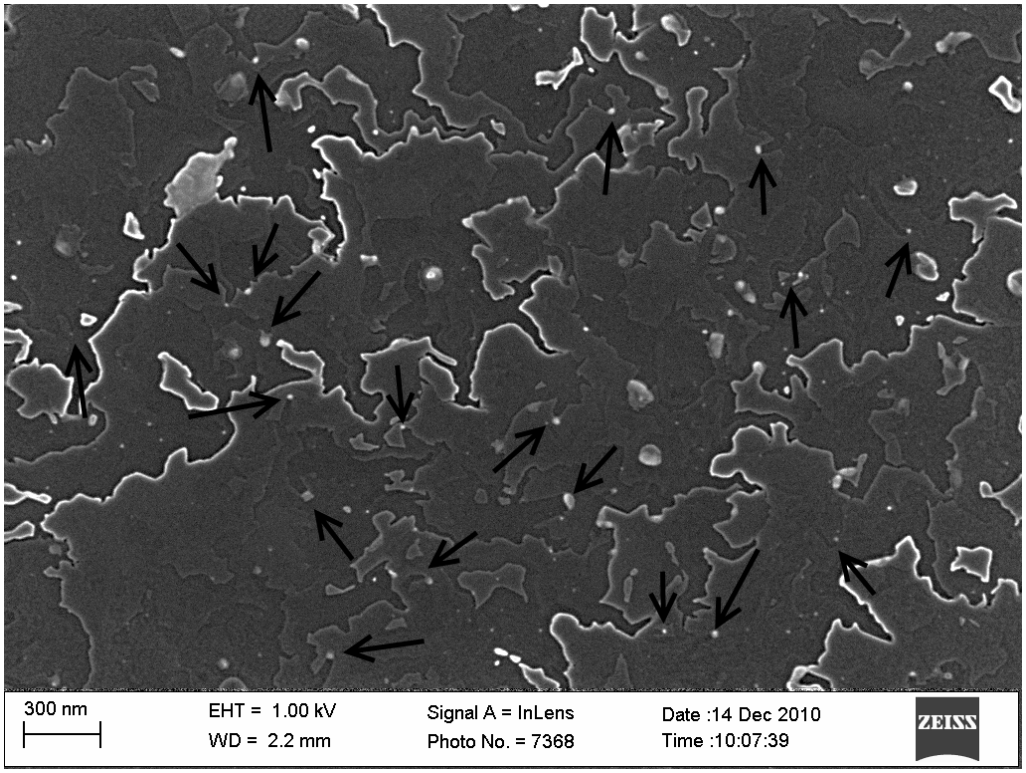

Figure 6-51: Catalyst particle activity 1 (75 000x)

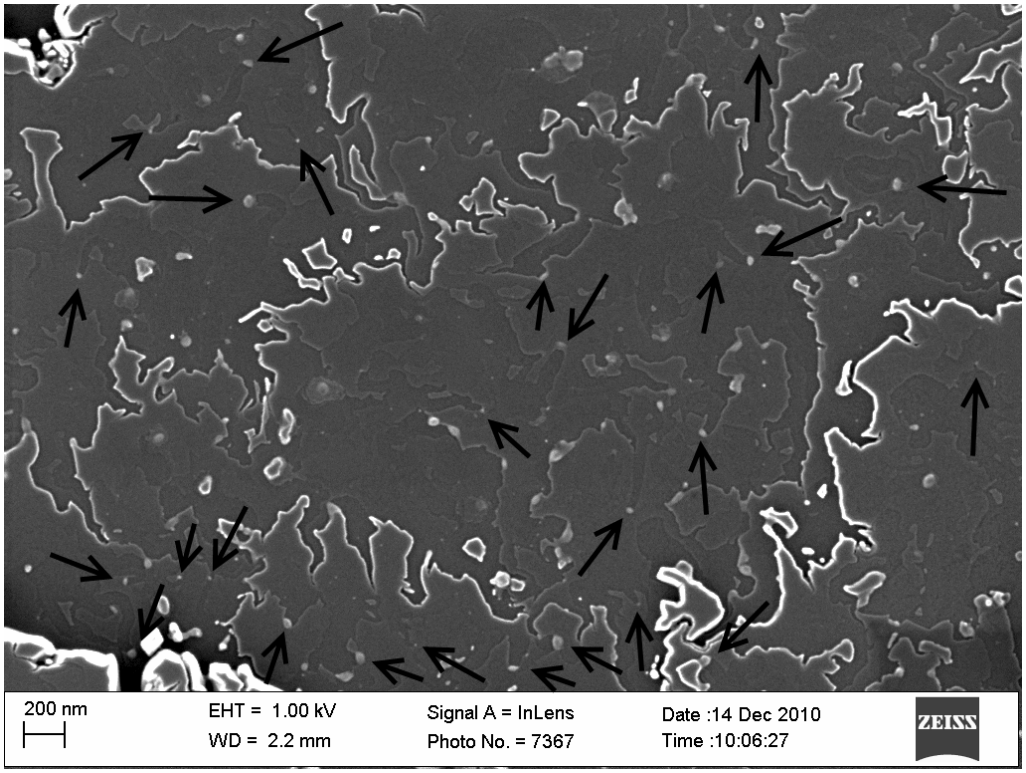

Figure 6-52: Catalyst particle activity 2 (60 000x magnification)

Catalytic pitting is a slightly more difficult behaviour to characterise since in some cases it is impossible to determine whether the pits are caused by minute catalytic particles or by lattice defects. Thus in this investigation any pitting behaviour is assumed to be independent of the source of the pits. Instead, the pits are assumed to exist at the start of the oxidation and to grow only as oxidation proceeds. Their effect on the conversion function is therefore accounted for by active surface area development, rather than by direct catalytic oxidation, as discussed in the previous chapter.

6.2 Analytical catalyst model

As a starting point for modelling the catalytic action of impurities, the model suggested by Ranish and Walker [340] is reviewed and adapted for the case of the ideal disc-shaped graphite flake. This model assumes that discrete, spherical catalyst particles propagate straight channels towards the centre of the circular disc. As a channel is formed, the walls of the channel are oxidised by the uncatalysed reaction. This leads to the formation of triangular channels in the graphite, as shown in Figure 6-53. All the while the outer edge of the flake is also subjected to uncatalysed oxidation, shrinking the disc, while the basal plane is left intact.

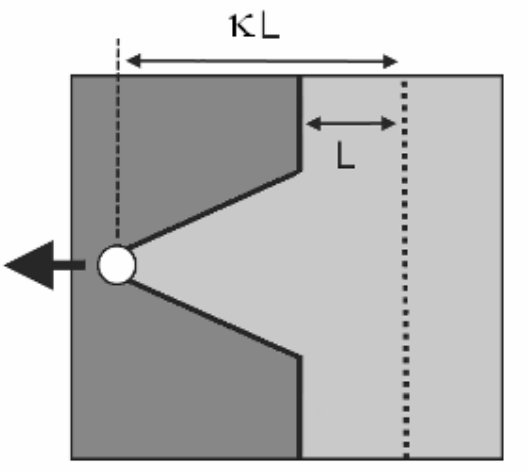

Figure 6-53: Catalyst particle model

These catalyst particles are randomly distributed along the outer circumference of the particle, at varying heights. When the catalysts have proceeded to such an extent that the walls of adjacent channels touch, the authors designate this point as the achievement of steady state roughness. This value is calculated as the point at which the pore mouth width multiplied by the average number of catalyst particles at a given height is equal to the circumference of the disc. All measured values are reported relative to this point and no attempt is made to model the particle behaviour beyond this point. Instead, to understand the complete burn-off behaviour and extend this model beyond the point of steady state roughening, a few assumptions are made.

Firstly, the catalyst particles are approximated as point particles, i.e. effectively zero diameter. This simplifies the model in terms of not only particle collisions, but also geometric considerations. Furthermore, the graphite flake is approximated as a disc with a height equal to the size of the catalyst particle. That is to say, all the catalyst particles act at a single level of the disc and the channel height is equal to the full height of the particle. This is equivalent to the previous approach in assuming that the entire particle is approximated by using only the horizontal disc slice where the pore mouths first coalesce. If required, the model could be extended to take the average behaviour of several slices with varying catalyst contents to achieve a more accurate picture of the behaviour of the entire particle. However, it should be noted that if the catalyst particles are randomly and homogeneously distributed along the particle circumference, all slices should have same behaviour on the whole.

The only adjustable parameters in the model are the uncatalysed reaction rate and the catalysed reaction rate. These two values determine how quickly the disc circumference recedes and also fixes the depth of the triangular channel that is formed by the catalyst particle. This subsequently sets the angle of the catalyst channel wall to the circumference of the disc. When the walls from adjacent channels meet, the pinnacle of this triangle will effectively be undergoing uncatalysed oxidation from two directions simultaneously. The true edge-recession rate, i.e. the rate at which this pinnacle recedes, can be calculated from simple geometric considerations to ensure that the recession of each wall that comprises the pinnacle recedes at the uncatalysed rate.

Thus the entire progression of conversion can be fully represented analytically simply by geometric analysis. As a starting point, ten catalyst particles are evenly distributed along the circumference of a graphite disc. The catalyst particles proceed towards the centre of the flake, while the channel walls and disc circumference undergo uncatalysed oxidation. A ratio of 3.5 for the rate of catalysed to uncatalysed reaction is used. This leads to the creation of triangular channels in the graphite similar to those observed in the real graphite. A visual representation of the progression of such a model is shown in Figure 6-54, for a disc with ten catalyst particles.

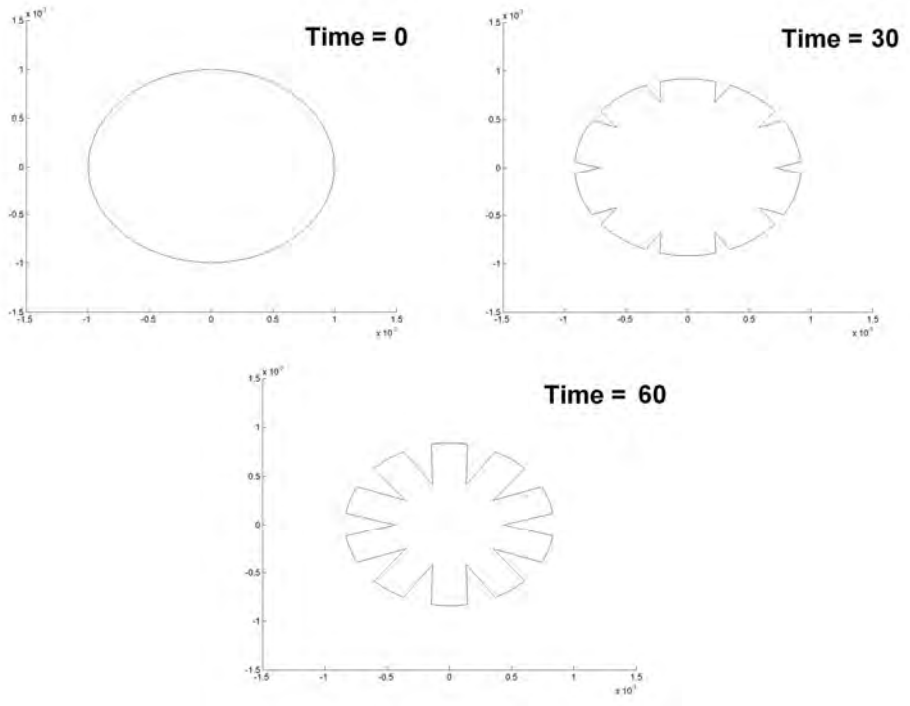

Figure 6-54: Analytical model progression

Of special interest is the case where the number of catalyst particles is increased such that pore coalescence occurs and steady state roughness is achieved. An example of such a case is shown in Figure 6-55. The calculated conversion function for this case is shown in Figure 6-56.

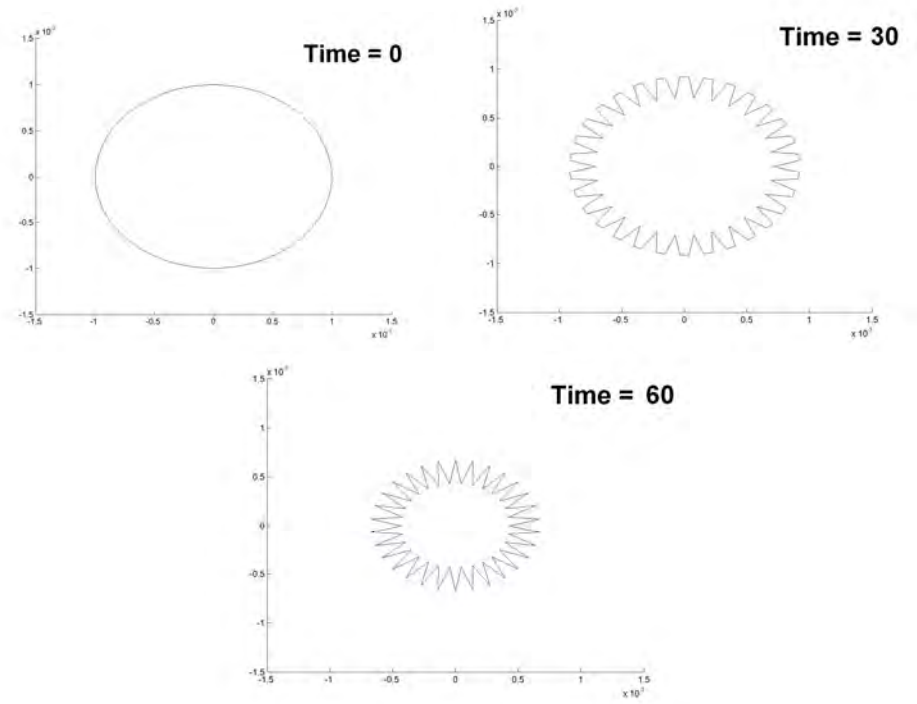

Figure 6-55: Analytical model progression with high catalyst content

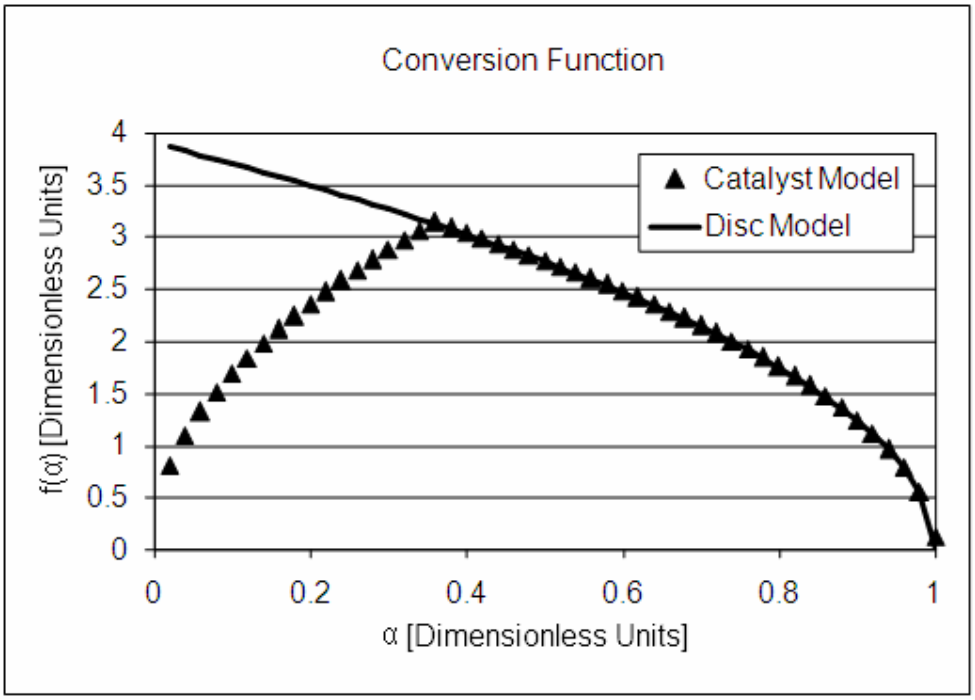

Figure 6-56: Analytical model conversion function

For comparative purposes, the analytical model for a disc with no catalyst is also shown in the figure. It is apparent that the reaction rate undergoes a rapid

acceleration. This is expected because a large amount of additional surface area is created by the catalyst channels. At a conversion of just below 40%, i.e. $\alpha = 0.4$, the channel walls coalesce and steady state roughness is achieved. It is interesting to note that beyond this point the model conforms to the ideal, uncatalysed disc shape. Thus beyond the point where steady state roughness is achieved, the intrinsic flake geometry governs the development of the active surface area. However, the reaction rate is much higher than it would be for an uncatalysed disc.

Consider that for a given uncatalysed reaction rate, the catalysed reaction rate will fix the angle of the formed catalyst channel. The higher the rate, the steeper the channel and the closer the pore mouth angle gets to being perpendicular with the edge. When the channels coalesce, the angle between them will determine the rate at which the pinnacle recedes. The steeper this angle, the higher the overall edge-recession rate. In fact, it can be shown analytically that the edge-recession rate that is achieved at this point is simply equal to the catalytic oxidation rate.

This has a direct implication for the activation energy of the composite particle. To model the temperature dependence of this system, two hypothetical activation energies may be selected for the catalysed and uncatalysed cases, e.g. 150 and 250 kJ/mol respectively. Assuming the original simulation was representative of the reaction at, e.g. 750 ºC, the relative increases in the two reaction rates can be calculated for reaction temperatures of 800 and 850 ºC. Using these calculated values, the unscaled reaction rate curves may be determined. These are shown in Figure 6-57.

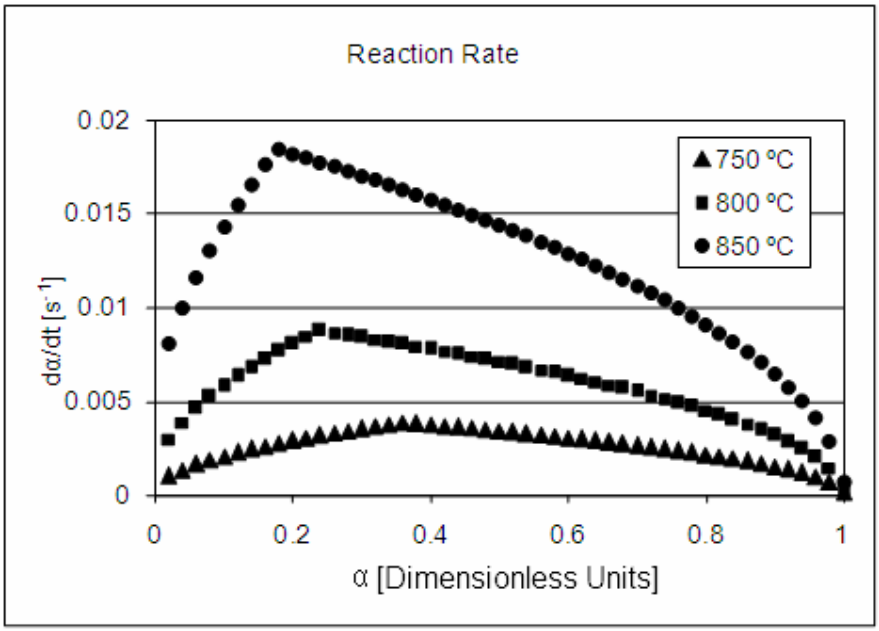

Figure 6-57: Temperature dependence of reaction rate

If a simple Arrhenius-type temperature dependence for the system as a whole is assumed, an arbitrary pre-exponential scaling factor may be selected. If the catalysed activation energy of 150 kJ/mol is used, the scaled conversion function curves may be constructed as shown in Figure 6-58.

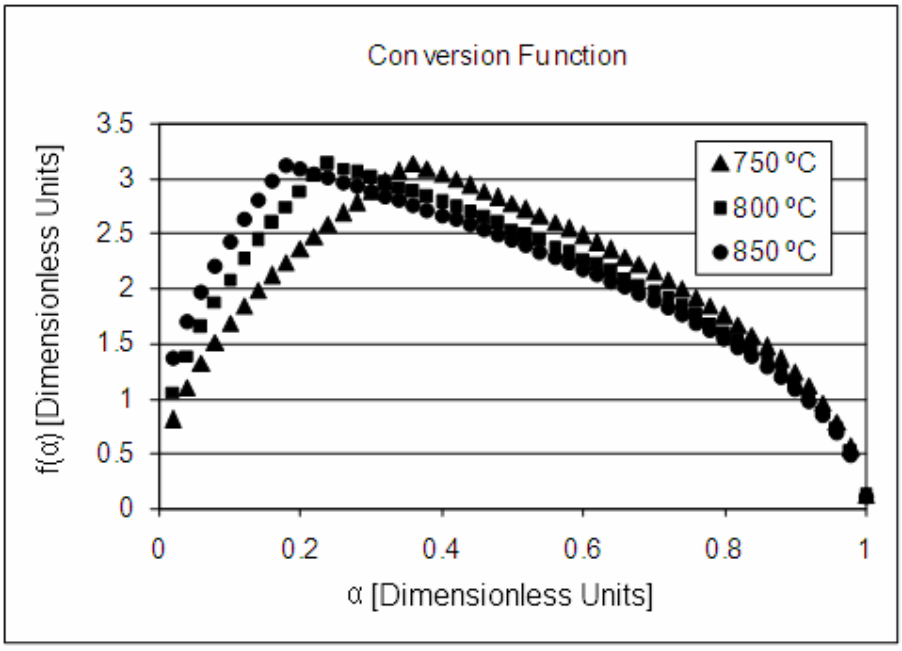

Figure 6-58: Scaled conversion functions

The peak reaction rates are perfectly compensated for the temperature difference in the model runs. This reinforces the idea that the reaction rate is governed solely by the catalysed reaction rate and hence the activation of the entire system is determined solely by the catalytic activation energy. There is, however, a small change in the shape of the conversion function. For higher temperatures, the conversion required to reach steady state roughening is reduced. Intuitively, this makes sense since the catalysed reaction rate is higher at a higher temperature, the catalyst particles penetrate the disc faster and channel coalescence occurs sooner.

Thus this analytical model provides three important insights into catalyst behaviour. Firstly, beyond the point of steady state roughness the conversion function of a particle under catalytic oxidation is the same as that for a particle with no catalyst. That is to say when steady state roughness is achieved, the inherent geometry of the particle governs the oxidation rate, i.e. from this point onward the conversion functions for the uncatalysed and catalysed particles will be exactly the same. Secondly, the reaction rate achieved at steady state roughness and beyond is equal to the catalysed reaction rate due to channel coalescence. This is indicated by the factor of roughly 3.5 by which the disc model has to be multiplied to conform to the catalysed reaction curves in Figure 6-56 and Figure 6-58, which was the ratio of the catalysed oxidation rate to the uncatalysed oxidation rate used in the simulation. Finally, the activation energy of a particle undergoing catalysed and uncatalysed oxidation is simply the catalysed activation energy.

These conclusions apply to the extremely simplified case of a single slice of an ideal disc with catalyst particles only channelling towards the centre of the disc. When comparing this situation to the experimentally observed behaviour it is clear that a more accurate representation of the random, erratic movement of real catalyst particles is needed.

6.3 Probability-based simulation of catalyst action

A very wide variety of catalytic behaviours is observable on the as-received graphite. Modelling all of these and linking them to an underlying mechanism would be an extremely difficult task. Instead, the dominant behaviour,

namely the highly erratic, almost fractal-like surface roughening, was chosen as the objective for simulation. This effect is known to be caused by a large number of small catalytic particles moving in a random walk along the flake edge or at basal steps. The probability-based simulation developed in Section 5.6 can easily be extended to include the action of a randomly moving catalytic particle.

The catalyst particles act independently from the bulk material, tracing a random walk into the graphite plane. They move freely and at a rate higher than the recession of the uncatalysed graphite edge. Individual catalyst particles may be simply approximated as subelements within the finite element grid and randomly distributed over a given surface geometry. As an example, see the disc with particles indicated by the red circles in Figure 6-59, enlarged for easier visualisation.

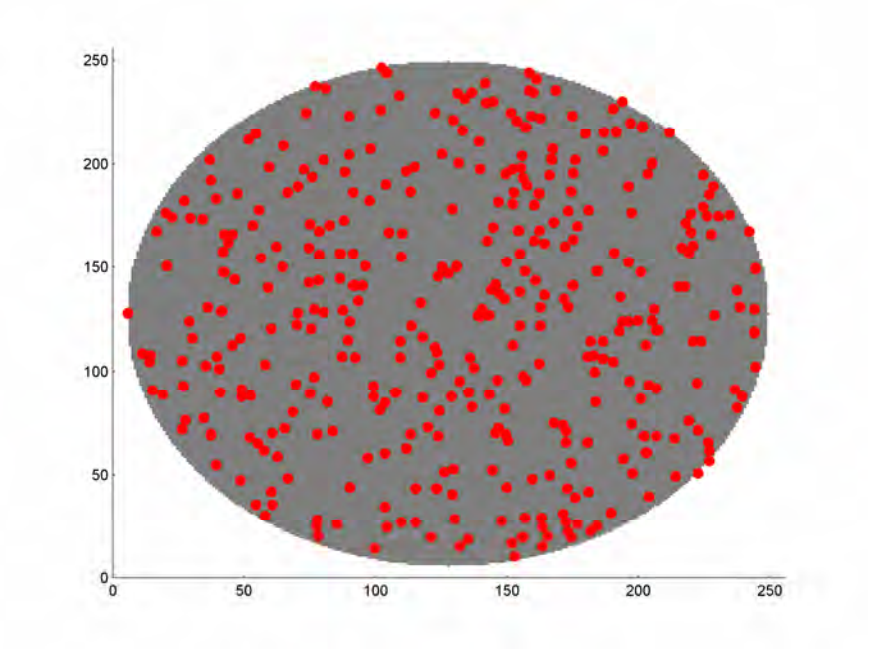

Figure 6-59: Catalyst distribution on disc

These subelements are free to move into any adjacent grid location that has a graphite particle present, removing it from the simulation as if it had been oxidised. Whether a catalyst particle has moved is determined by comparing a random number to a fixed reactivity or reaction probability and if the number is smaller than this probability, the catalyst is deemed to have reacted away the graphite. This is identical to the process used for the uncatalysed reaction, only a single probability exists which is independent of the number of sides that are

exposed. The only real requirement is that the catalyst particle must be adjacent to an unreacted graphite subelement.

This implies that the simulation has two different reaction probabilities, namely for the catalysed vs. uncatalysed reactions. This allows easy correlation of the model to an observed catalysed to uncatalysed reaction rate ratio. As mentioned previously, for a fairly straight channel, this can be approximated as the ratio of the distance to the channel tip divided by half the channel width at its origin. However, these rates vary widely, depending on particle size and catalyst type. Based on Figure 6-20, a ratio of 2.5 was calculated. This is much lower than the values typically reported [340]. Instead, a value of 20 will be used in this simulation.

The catalyst concentration can be determined by utilising the catalyst density. Fortunately, in this case the catalyst is sodium carbonate which has a density of 2.25 g/cm^3, practically identical to that of graphite. Thus the mass concentration of catalyst is equal to the ratio of catalytic subelements to graphitic subelements. This is subject to the assumption that the catalyst particle is the same size as the graphitic layer into which it is channelling. For very thin layers this is approximately true, but for the macro behaviour observed in Figure 6-50 it appears that very small catalyst particles are capable of inducing damage in edges far larger than the particles themselves.

In the previous section the flake thickness used to calculate the simulation parameters was 20 µm, which is significantly larger than the edge noticeable in Figure 6-50. Thus the calculation of catalyst concentration in this fashion overestimates the amount of catalyst needed to induce the equivalent behaviour in a real flake. Considering the fact that the observed edge structures are at best no more than 200 nm, the catalyst concentrations are incorrect by a factor of at least 100. For the simulations with catalysts, concentrations of around 2.5% were therefore used to simulate the real contamination levels of 250 ppm.

To determine in which direction the catalyst particle moves, a second random number generator is used to ensure that the catalyst follows a random walk. A fully surrounded catalyst particle has eight possible movement directions; each is assigned a number between one and eight. Based on this, a random integer number between one and eight is generated to determine which direction is chosen. This is done by generating a random number between zero and eight

and rounding up. If another catalyst or an empty space occupies one or more of the directions, the generated number is reduced by the appropriate amount. Hence in this simple model, catalyst particles cannot collide.

The scale of the edge roughening relative to the size of the flake is an important factor when trying to simulate this behaviour. This is affected by the relative rates of the catalysed and uncatalysed reactions, which in turn are dependent on the reaction temperature, as well as on the overall particle size of the graphite flake under consideration. As a starting point, a circular disc was contaminated with catalyst, as shown in Figure 6-59, and allowed to react. The time-based progression of this simulation is shown in Figure 6-60.

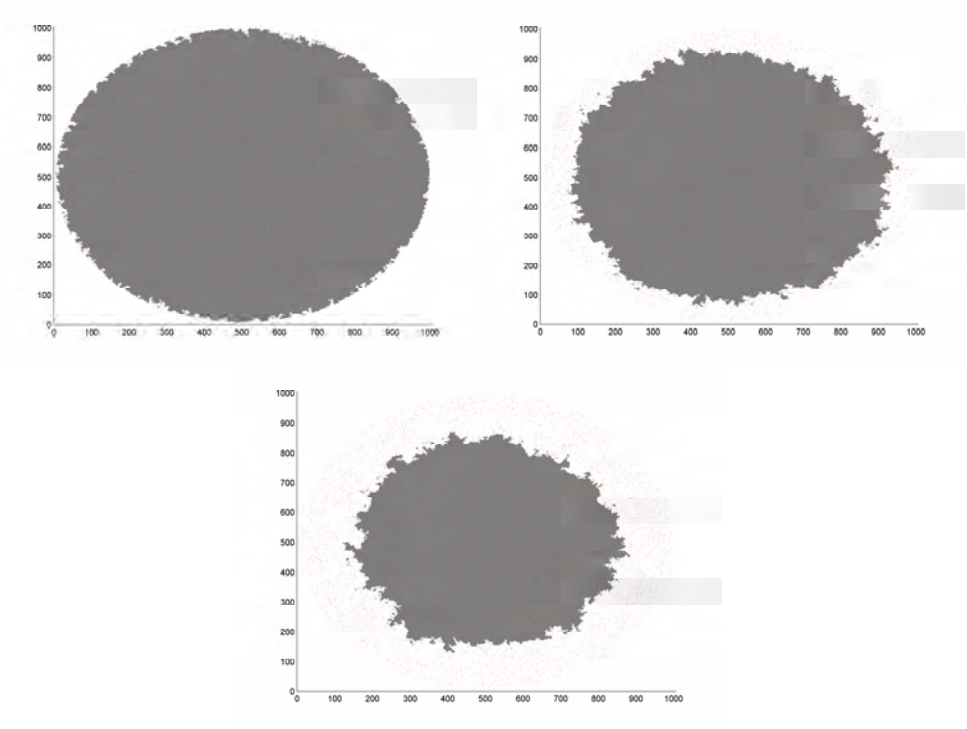

Figure 6-60: Probability-based disc model with catalyst contamination

Initially, small channels are formed along the disc edge which grow over time. Particles are continually deactivated by becoming stranded on very small graphite islands due to their rapid, random movement. However, new catalytic particles are simultaneously activated via exposure to new open-edge regions. Throughout the simulation the disc retains its roughly circular shape, undergoing both catalysed and uncatalysed oxidation at the edge. The persistent activation

and deactivation ensures continuous catalytic activity at the disc edge, leading to the fine edge structure that can be observed in Figure 6-61.

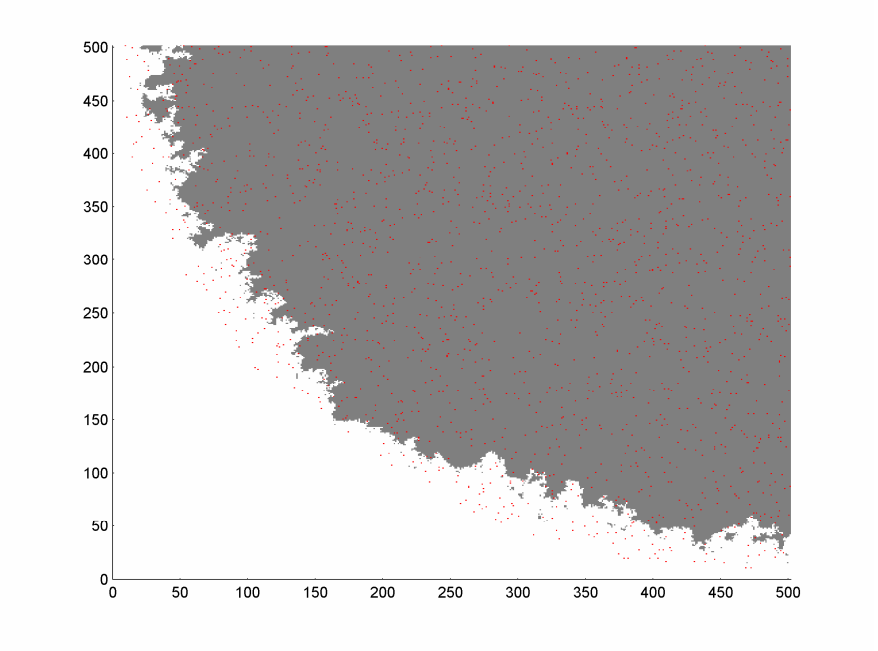

Figure 6-61: Simulated edge roughening

A myriad of fine channels are present, evenly distributed along the flake edge. When the edge is examined more closely, the random, erratic nature of the channels becomes clearly visible, as shown in Figure 6-62.

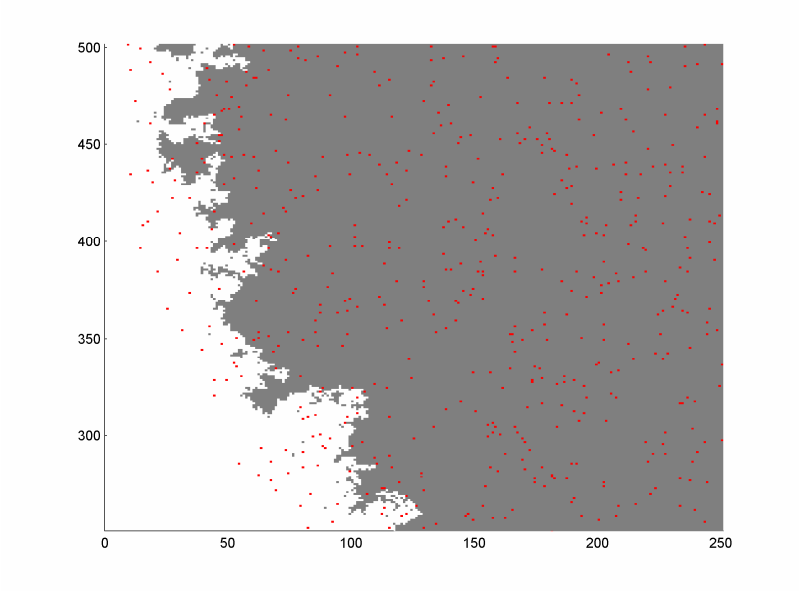

Figure 6-62: Simulated catalyst channelling

By comparison with Figure 6-47 to Figure 6-52, one can see that the simulation visually represents real behaviour very satisfactorily. Finally, the kinetic behaviour of the catalytic simulation can be evaluated. As expected, the behaviour is very similar to that of the analytical model shown in Figure 6-56. The conversion function for this simulation is compared with that of the uncatalysed disc, multiplied by a factor of three, in Figure 6-63.

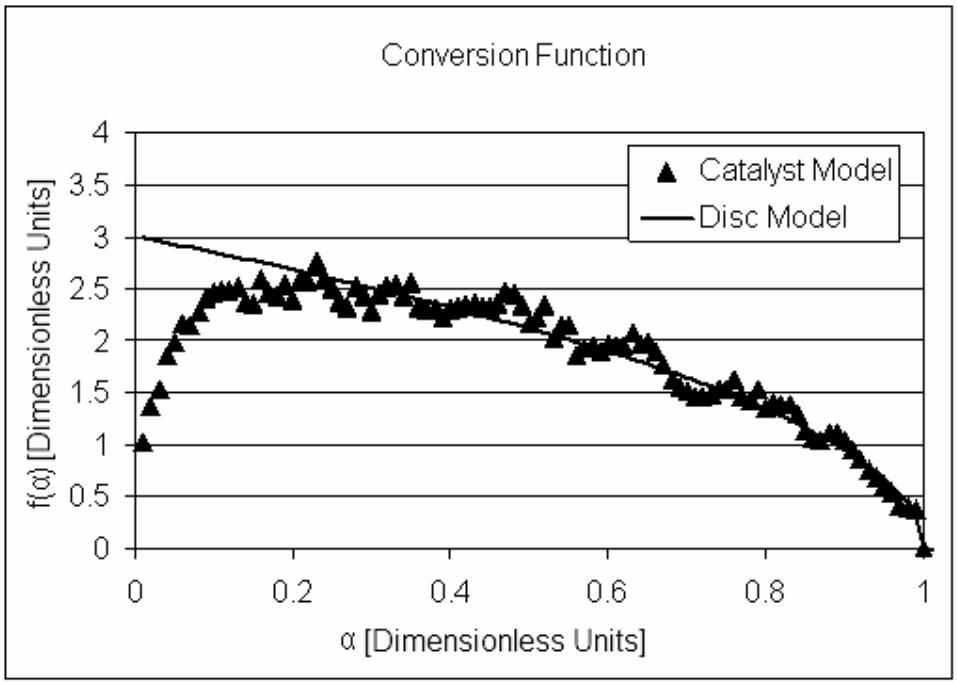

Figure 6-63: Analytical model conversion function

As expected, the observed conversion function undergoes an extended roughening period due to the catalytic action, before attaining a pseudo-steady state. Beyond this point the inherent geometry takes over and the conversion function is governed by the disc-like behaviour, albeit at three times the original reaction rate. This is in contradiction to the observation in the previous section that the reaction rate at this point should conform to the catalysed reaction rate since the ratio of catalysed to uncatalysed reaction rates used in this simulation was 20.

The discrepancy is caused by the random, erratic movement of the catalyst particles. In the previous model the particles simply channel straight to the centre of the graphite disc. In the current simulation the particles move randomly along the edge and thus not all catalytic oxidation movements

contribute directly to an effective decrease in the particle diameter. Instead, the true catalytic rate reducing the particle circumference is some average of these movements, in this case accelerating the edge-recession rate by a factor of only around three. Furthermore, due to this random, erratic nature of the catalytic channelling, the simulation shows a significant amount of noise or variability. For this reason the average of three repeat simulations is used in subsequent comparisons.

To understand the temperature-based behaviour of the simulated catalyst, the analysis used for the analytical model may be repeated for this simulation. The exact same activation energies and temperatures are assumed and the resulting reaction rate curves are shown in Figure 6-64.

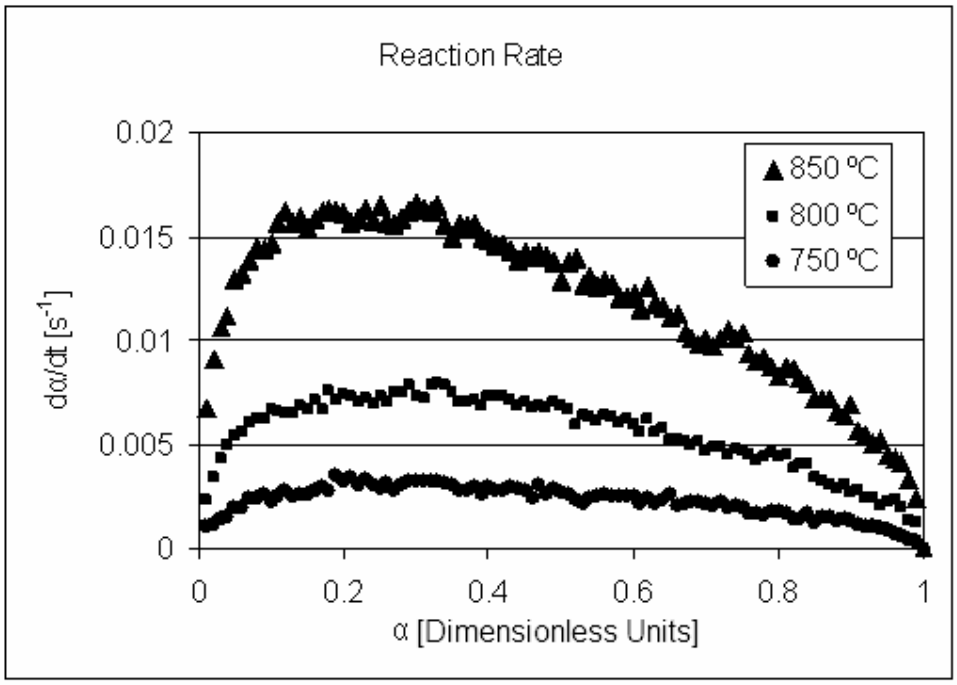

Figure 6-64: Temperature dependence of simulated reaction rate

If a simple Arrhenius-type temperature dependence for the system is again assumed, an arbitrary pre-exponential scaling factor may be selected. If the catalysed activation energy of 150 kJ/mol is used, the scaled conversion function curves may be constructed as shown in Figure 6-65.

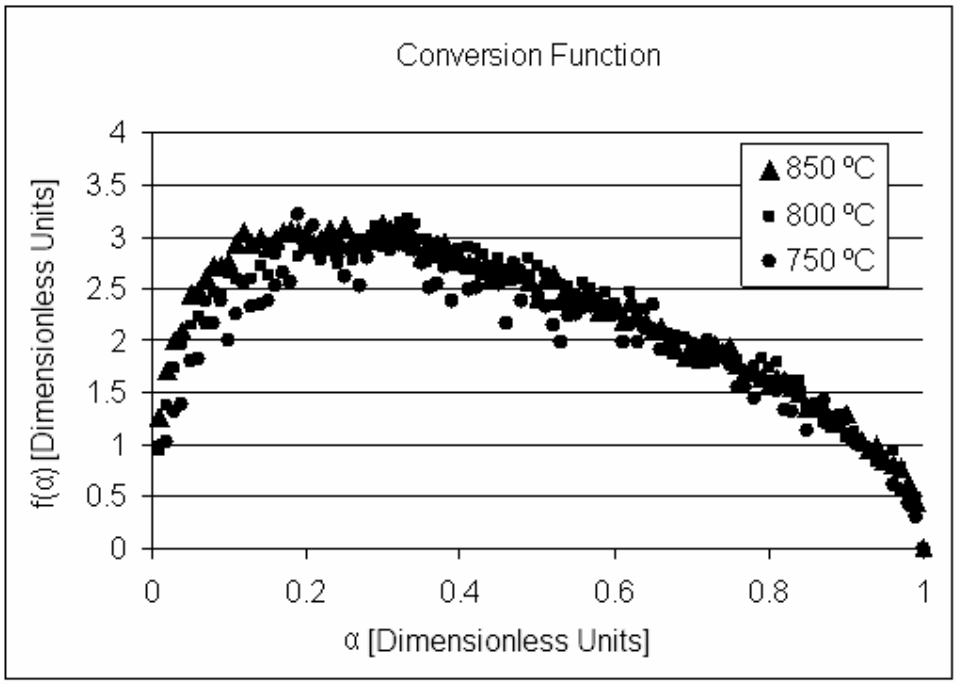

Figure 6-65: Scaled conversion functions for simulation

Again, a single activation energy, equivalent to that of the catalysed reaction, is sufficient to describe the composite system. In this case, however, due to the random, erratic nature of the edge roughening, the shift in the peak reaction rate, i.e. the point at which steady state roughness is achieved, is much less pronounced. In this case the conversion behaviour is virtually independent of temperature. It is also important to note that the roughening effect achieves steady state fairly rapidly compared with the analytical model, i.e. below conversions of 10%. Thus despite the visually large difference between the analytical model and the random, erratic nature of the simulated catalyst behaviour, the conclusions are the same.

These observations lead to a few important conclusions regarding the catalytic oxidation of graphite:

- Geometries undergoing catalytic oxidation are expected to undergo an initial roughening period as the catalyst creates a roughened edge. The extent of this initial roughening period will depend heavily on the channelling behaviour and catalytic activity. For the random, erratic behaviour of real catalysts observed, this effect may be expected to occur very rapidly.

- After the initial roughening period has been overcome, the inherent geometry of the particle under consideration takes over. The conversion function of this inherent geometry has the same shape as is observed for uncatalysed oxidation.
- The temperature-based behaviour of the composite system undergoing both catalysed and uncatalysed oxidation can be described by a single activation energy, attributable to the catalysed oxidation only.
- Thus the effect of catalytic impurities may be broadly thought of as simply catalysing the inherent geometry of the graphite flake. This is done by creating additional active surface area, via random, erratic channelling, which accelerates the uncatalysed reaction rate in accordance with some fraction of the catalysed reaction rate.

These conclusions may be verified for the more complex geometries mentioned in the previous section by contaminating the simulated, purified RFL graphite (PRFL) structure with catalyst and comparing this behaviour with the uncatalysed, experimental behaviour. As can be seen in Figure 6-66, the active surface area and hence the conversion function rapidly increase until steady state roughening is achieved. Beyond this point the original behaviour takes over.

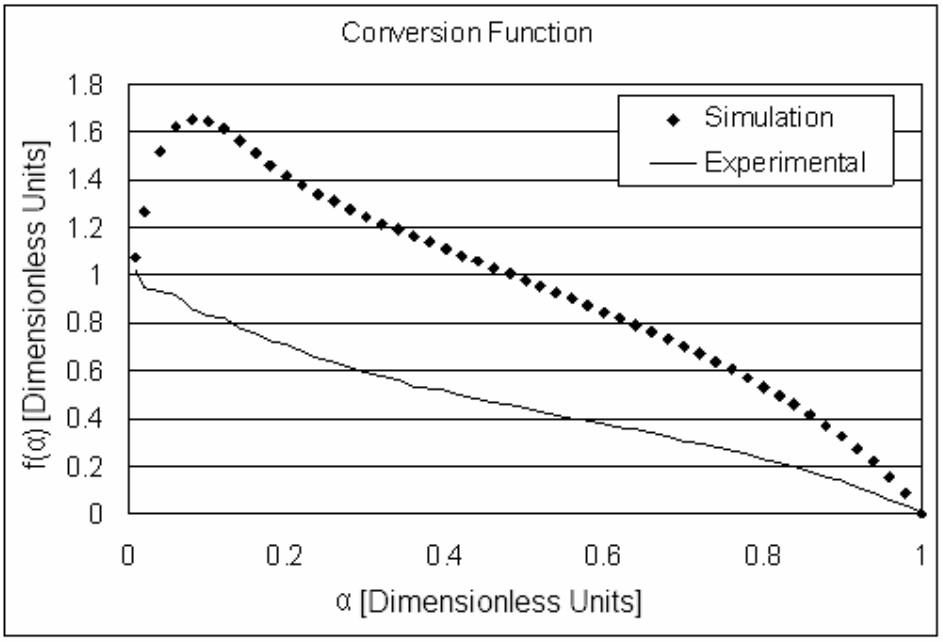

Figure 6-66: Scaled conversion function for catalysed simulation

This is more readily observable if the entire simulated conversion function is multiplied by a factor of 0.5. In this case conformance to the original, uncatalysed experimental data, beyond conversions of around 10%, is clearly evident in Figure 6-67.

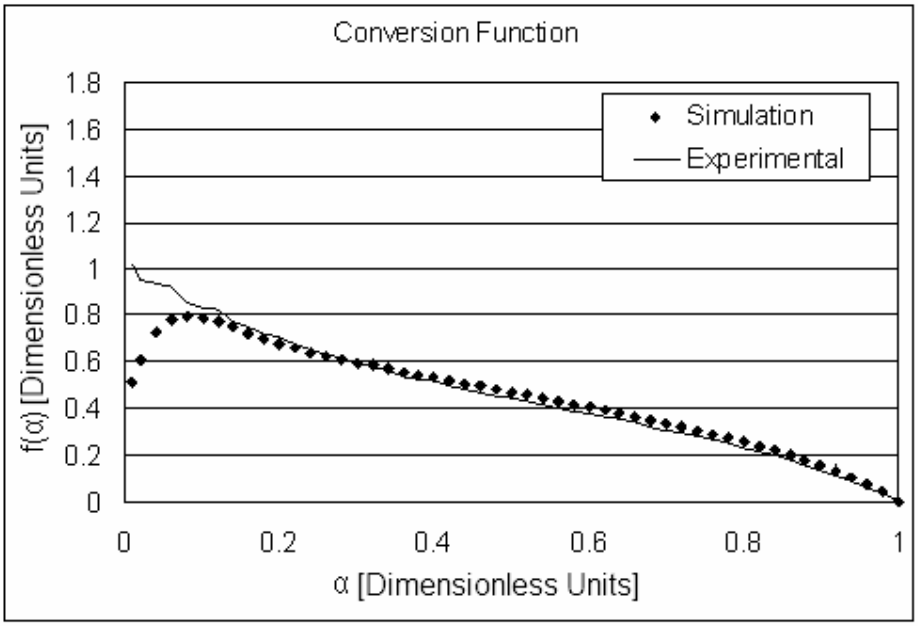

Figure 6-67: Rescaled conversion function for catalysed simulation

Thus the only effects of the catalyst on the original conversion behaviour are the creation of an induction period and an increase in the overall reaction rate by a factor of two. It may be noted that the contaminated, purified material does not exhibit the initial roughening period expected from the simulated behaviour. However, comparison of the kinetic constants, in this case the estimated initial ASA, indicates that for a given temperature, the reaction rate of the contaminated sample will be higher than that of the uncontaminated sample by a factor of 343. This increase in reactivity is far more than the observed doubling of the reaction rate in the simulation. Due to limitations in the time allowed for the simulation, the use of such a high ratio is not possible. For such a highly reactive catalyst, it is entirely conceivable that the induction period is so rapid as not to be directly observable. Hence the contaminated and uncontaminated conversion functions of the real samples appear to be identical.